J. Fluid Mech. (1968), *vol.* 32, *part* 3, *pp.* 569–607
Printed in Great Britain

On the existence and structure of inertial boundary currents in a stratified ocean

By S. L. SPIEGEL† AND A. R. ROBINSON
Pierce Hall, Harvard University

(Received 12 September 1967)

An investigation is made of the properties of inertial boundary currents in a stably stratified, inviscid, non-diffusive ocean. The Boussinesq and β-plane approximations are adopted. The formalism developed by Robinson (1965) is used: the equations are transformed so that density replaces the vertical co-ordinate as an independent variable, and after a suitable non-dimensionalization of variables, the various fields are expanded as power series in the downstream co-ordinate η. The motion is shown to conserve potential vorticity. The equations and boundary conditions are obtained to order η^2. Solutions are obtained in the region of formation of the coastal jet (i.e. the case of no mass flux through the plane $\eta = 0$) for several cases in which the potential vorticity function depends on stream function and density in a simple way. For these cases, it is found that in a constant depth ocean, a boundary current can exist only if the geostrophic drift at the boundary-layer edge is westward at all depths. This constraint is relaxed if the depth increases rapidly enough in the downstream (northward) direction. For slopes just in excess of the critical value, a deep onshore counter-current is predicted. Solutions of the first-order problem, using realistic values of the various parameters, have been computed and are found to be in qualitative agreement with observed features of the Florida Current.

In an appendix, it is shown that the constraint of westward geostrophic drift at all levels must hold in a flat-bottomed ocean for arbitrary potential vorticity distributions consistent with stable stratification.

1. The inertial boundary current

1.1. *Introduction*

A model for the study of inertial currents in a continuously stratified ocean has been discussed by Robinson (1965, hereafter referred to as IC). In that paper the formalism proposed was applied to the problem of the formation of a coastal jet (Gulf Stream problem) for certain simple potential vorticity distributions in a constant depth ocean. It was shown that a western boundary current of constant potential vorticity requires an influx of fluid at all levels at its seaward edge. It is the object here to extend that analysis by (i) considering a wider class of potential vorticity distributions, (ii) examining the effects of downstream depth

† Present address: Department of Meteorology, Massachusetts Institute of Technology, Cambridge, Mass.

variations, and (iii) carrying the downstream co-ordinate expansion of fields (intrinsic to the formalism) to the next highest order.

Potential vorticity functionals that depend linearly on stream function but are independent of density are studied. These distributions correspond to seaward edge geostrophic drifts that are simply stratified but have a variety of downstream behaviours. Functionals proportional to the square of the density, corresponding to a basic thermocline structure, are also examined. The purpose is to determine what bottom topographies, and (seaward) velocity and density distributions allow an inertial boundary jet to form, and to compare the class of allowed interior-jet systems to the real oceans. Accordingly, the resultant jet structures are computed for several cases of geometry and geostrophic drift, and for one of these, comparison is made with Florida Current sections.

1.2. *Statement of the problem*

The problem to be considered is that of the formation of an inertial jet along the (straight) lateral boundary of a stratified, inviscid, non-diffusive ocean. The Boussinesq, hydrostatic and β-plane approximations are employed. In IC, the equations of the model are given, a transformation is made whereby density replaces physical height as an independent variable, and a suitable non-dimensionalization of variables is performed; the reader is referred to IC for a detailed discussion and for details of the notation.

Briefly, the various fields are expanded as power series in the downstream variable, e.g.

$$u(\xi, \eta, \theta) = \sum_{n=0}^{\infty} u_n(\xi, \theta)\, \eta^n/n!$$

(note that this definition differs by a factor $1/n!$ from that in IC). For the case $v_0 \equiv 0$, the equations (2.1)–(2.7) of IC in non-dimensional form, can be written, to indicated order in η:

$$(2.1) \rightarrow \begin{cases} O(\eta^0) & \Pi_{0\xi} = v_0 \equiv 0, \quad (1.1) \\ O(\eta^1) & -v_1 + \Pi_{1\xi} = 0, \quad (1.2) \\ O(\eta^2) & -v_2 - 2\beta^* v_1 + \Pi_{2\xi} = 0, \quad (1.3) \end{cases}$$

$$(2.2) \rightarrow \begin{cases} O(\eta^1) & u_0 + \Pi_1 = 0, \quad (1.4) \\ O(\eta^2) & u_0 v_{1\xi} + v_1^2 + u_1 + \beta^* u_0 + \Pi_2 = 0, \quad (1.5) \end{cases}$$

$$(2.3) \rightarrow O(\eta^m) \quad \zeta_m + \Pi_{m\theta} = 0, \quad (1.6)$$

$$(2.4) \rightarrow O(\eta^0) \quad (u_{0\xi} + v_1)\, \zeta_{0\theta} = 0, \quad (1.7)$$

$$(2.5) \rightarrow \begin{cases} O(\eta^0) & w_0 = u_0 \zeta_{0\xi} + v_0 \zeta_1, \quad (1.8) \\ O(\eta^1) & w_1 = u_0 \zeta_{1\xi} + v_1 \zeta_1, \quad (1.9) \\ O(\eta^2) & w_2 = u_0 \zeta_{2\xi} + 2u_1 \zeta_{1\xi} + 2v_1 \zeta_2 + v_2 \zeta_1, \quad (1.10) \end{cases}$$

$$(2.6) \rightarrow \begin{cases} O(\eta^0) & u_0 \zeta_{0\theta} = -\psi_1, \quad (1.11) \\ O(\eta^1) & u_1 \zeta_{0\theta} + u_0 \zeta_{1\theta} = -\psi_2, \quad (1.12) \\ O(\eta^0) & \psi_{0\xi} = v_0 \zeta_{1\xi} \equiv 0, \quad (1.13) \\ O(\eta^1) & \psi_{1\xi} = v_1 \zeta_{0\theta}, \quad (1.14) \end{cases}$$

$$(2.7)\rightarrow\begin{cases}O(\eta^0) & 1=\zeta_{0\theta}P_0, \quad (1.15)\\ O(\eta^1) & v_{1\xi}+\beta^*=\zeta_{0\theta}P_I\psi_1+\zeta_{1\theta}P_0, \quad (1.16)\\ O(\eta^2) & v_{2\xi}=\zeta_{0\theta}(P_I\psi_2+P_{II}\psi_1^2)+2\zeta_{1\theta}P_I\psi_1+\zeta_{2\theta}P_0. \quad (1.17)\end{cases}$$

Here,
$$P_N=\left.\frac{\partial^N P}{\partial\psi^N}\right|_{\psi=\psi_0}$$
and for $v_0=0$, it is proper to take $\psi_0=0$ whence $P_N=P_N(\theta)$.

The boundary conditions must be consistently transformed and expanded: the reader is referred to IC for details of the first-order derivation; the second-order conditions follow similarly. The notation differs from that of IC in that the (non-dimensional) bottom height is here denoted by $\zeta=R_1\eta+\frac{1}{2}R_2\eta^2+\ldots$, with the R_n independent of ξ and the second zero subscript, indicating the ξ-independency of b_0 and h_0 imposed by the $v_0=0$ constraint, is suppressed. The conditions are:

(a) At the free surface ($\theta=h_0+h_1(\xi)\eta+\frac{1}{2}h_2(\xi)\eta^2+\ldots$)

$$O(\eta^0) \qquad w_0=0, \quad (1.18)$$
$$O(\eta^1) \qquad w_1=0, \quad (1.19)$$
$$O(\eta^2) \quad w_2+2h_1w_{1\theta}=0. \quad (1.20)$$

(b) At the bottom ($\theta=b_0+b_1(\xi)\eta+\frac{1}{2}b_2(\xi)\eta^2$)

$$O(\eta^0) \qquad w_0=R_1v_0\equiv 0, \quad (1.21)$$
$$O(\eta^1) \qquad w_1=R_1v_1, \quad (1.22)$$
$$O(\eta^2) \quad w_2+2b_1w_{1\theta}=R_1v_2+2R_2v_1. \quad (1.23)$$

(c) At the coast
$$u_n=0, \quad \text{all } n. \quad (1.24)$$

(d) At the boundary-layer edge
$$v_n \quad \text{and} \quad w_n\rightarrow 0 \quad \text{exponentially.} \quad (1.25)$$

1.3. *The $v_0=0$ coastal jet*

Equations (1.1)–(1.14) can be utilized to write the variables u, v, w and ζ in terms of the Π-field:

$$u_0=-\Pi_1, \quad (1.26)$$
$$u_1=-\Pi_2+\Pi_1(\Pi_{1\xi\xi}+\beta^*)-\Pi_{1\xi}^2, \quad (1.27)$$
$$v_0=\Pi_{0\xi}\equiv 0, \quad (1.28)$$
$$v_1=\Pi_{1\xi}, \quad (1.29)$$
$$v_2=\Pi_{2\xi}-2\beta^*\Pi_{1\xi}, \quad (1.30)$$
$$w_0\equiv 0, \quad (1.31)$$
$$w_1=\Pi_1\Pi_{1\theta\xi}-\Pi_{1\theta}\Pi_{1\xi}, \quad (1.32)$$
$$w_2=\Pi_1\Pi_{2\theta\xi}+2\Pi_{1\theta\xi}[\Pi_2-\Pi_1(\Pi_{1\xi\xi}+\beta^*)+\Pi_{1\xi}^2]-2\Pi_{1\xi}\Pi_{2\theta}-\Pi_{1\theta}[\Pi_{2\xi}-2\beta^*\Pi_{1\xi}], \quad (1.33)$$
$$\zeta_0=-\Pi_{0\theta}, \quad (1.34)$$
$$\zeta_1=-\Pi_{1\theta}, \quad (1.35)$$
$$\zeta_2=-\Pi_{2\theta}. \quad (1.36)$$

These relationships are now substituted in the potential vorticity equations, (1.15)–(1.17), and the related boundary conditions. To zero order in η,

$$\zeta_0'(\theta) = -\Pi_0''(\theta) = \frac{1}{P_0(\theta)}, \tag{1.37}$$

with the appropriate boundary conditions (1.18) and (1.21) identically satisfied. Note from (1.37) that the requirement of stable stratification at $\xi \to \infty$, $\eta \to 0$ imposes the condition $P_0 > 0$.

The first-order equation and associated boundary conditions are:

$$\Pi_{1\xi\xi} + P_0 \Pi_{1\theta\theta} - \frac{P_I}{P_0^2}\Pi_1 = -\beta^*, \tag{1.38}$$

$$\Pi_1 = 0 \quad \text{at} \quad \xi = 0, \tag{1.39}$$

$$\Pi_{1\xi} \to 0 \quad \text{as} \quad \xi \to \infty, \tag{1.40}$$

$$\Pi_1 \Pi_{1\theta\xi} - \Pi_{1\theta}\Pi_{1\xi} = \begin{cases} R_1 \Pi_{1\xi} & \text{at} \quad \theta = b_0 \quad (1.41') \\ = 0 & \text{at} \quad \theta = h_0. \quad (1.42') \end{cases}$$

Since b_0 and h_0 are independent of ξ, a ξ-integration may be performed on (I.41′) and (I.42′). This yields the equivalent boundary conditions,

$$K_0(\Pi_{1\theta} + R_1) - \Pi_1 = 0 \quad \text{at} \quad \theta = b_0, \tag{1.41}$$

$$K_1 \Pi_{1\theta} - \Pi_1 = 0 \quad \text{at} \quad \theta = h_0 \tag{1.42}$$

(cf. IC equation (3.22*b*)). Here, K_0 and K_1 are constants of integration which, in conjunction with P_0, P_I, β^* and R_1, serve to specify completely the first-order flow. Physically, K_1 is the ratio of cross-stream velocity to downstream isotherm slope at the surface, and K_0 is the ratio of cross-stream velocity to the sum of downstream isotherm and bottom slopes at the bottom.

To second order,

$$\Pi_{2\xi\xi} + P_0 \Pi_{2\theta\theta} - \frac{P_I}{P_0^2}\Pi_2$$

$$= 2\beta^* \Pi_{1\xi\xi} + \frac{P_I}{P_0}\left\{\frac{1}{P_0}[\Pi_{1\xi}^2 - \Pi_{1\xi}(\Pi_{1\xi\xi} + \beta^*)] - 3\Pi_1 \Pi_{1\theta\theta}\right\} + \frac{P_{II}}{P_0^3}\Pi_1^2, \tag{1.43}$$

$$\Pi_2 + \Pi_{1\xi}^2 = 0 \quad \text{at} \quad \xi = 0, \tag{1.44}$$

$$\Pi_{2\xi} \to 0 \quad \text{as} \quad \xi \to \infty. \tag{1.45}$$

The boundary conditions expressed by (1.20) and (1.23), after being written in terms of the Π_n, may be integrated once over ξ after an appropriate grouping of terms and the use of (1.37), (1.41) and (1.42). The resultant conditions are:

$$K_0(\Pi_{2\theta} + R_2) - \Pi_2 = \Pi_{1\xi}^2 - 2P_0 \Pi_1 \left(\Pi_{1\theta\theta} + \frac{R_1}{K_0}\right) + L_0 \Pi_1^2 \equiv \hat{A}(\xi) \quad \text{at} \quad \theta = b_0, \tag{1.46}$$

$$K_1 \Pi_{2\theta} - \Pi_2 = \Pi_{1\xi}^2 - 2P_0 \Pi_1 \Pi_{1\theta\theta} + L_1 \Pi_1^2 \equiv \hat{B}(\xi) \quad \text{at} \quad \theta = h_0. \tag{1.47}$$

The quantities L_0 and L_1 are constants of integration. It will be found convenient to define a new variable $\hat{\Pi}(\xi, \theta)$ by the relation

$$\Pi_2 = \hat{\Pi} + \frac{1}{\Delta_0}[(\hat{B} - \hat{A})\theta + (K_0 - b_0)\hat{B} - (K_1 - h_0)\hat{A}], \tag{1.48}$$

where $\Delta_0 \equiv K_1 - K_0 - (h_0 - b_0) = K_1 - K_0 - 1$. Then $\hat{\Pi}$ satisfies the equations

$$\hat{\Pi}_{\xi\xi} + P_0 \hat{\Pi}_{\theta\theta} - \frac{P_I}{P_0^2} \hat{\Pi} = \{\text{right-hand side of (1.43)}\}$$
$$- \frac{1}{\Delta_0} [(\hat{B}'' - \hat{A}'')\theta + (K_0 - b_0)\hat{B}'' - (K_1 - h_0)\hat{A}'']$$
$$+ \frac{P_I}{P_0^2 \Delta_0} [(\hat{B} - \hat{A})\theta + (K_0 - b_0)\hat{B} - (K_1 - h_0)\hat{A}], \quad (1.49)$$

$$K_0(\hat{\Pi}_\theta + R_2) - \hat{\Pi} = 0 \quad \text{at} \quad \theta = b_0, \quad (1.50)$$

$$K_1 \hat{\Pi}_\theta - \hat{\Pi} = 0 \quad \text{at} \quad \theta = h_0. \quad (1.51)$$

In the event $\Delta_0 = 0$, it is better to make the substitution

$$\Pi_2 = \hat{\Pi}' - \tfrac{1}{2}(\hat{A} - \hat{B}) \cos \pi\theta - \tfrac{1}{2}(\hat{A} + \hat{B}) \cos 2\pi\theta \quad (1.48')$$

instead of (1.48); the function $\hat{\Pi}'(\xi, \theta)$ will also satisfy the desired boundary conditions (1.50) and (1.51).

2. Solutions for several classes of potential vorticity

The solutions to the above equations (1.37)–(1.51) will now be investigated for four different forms of the potential vorticity:

(i) $P = P_0 = 1$ (constant potential vorticity),

(ii) $P = 1 - \alpha^2 \psi$,

(iii) $P = 1 + \alpha^2 \psi$,

(iv) $P = P_0(\theta) \propto \theta^2$.

Inasmuch as the Gulf Stream may be rather well represented by a two-layer model with the potential vorticity of the upper layer taken as constant (Stommel 1965), or as a slowly varying function of stream function (Charney 1955), it can be expected that forms (i)–(iii) are capable of describing boundary currents of physical interest. Form (iv) is chosen because it can express a more realistic zero-order temperature profile than the linear gradient implied by a constant P_0 (taking that constant to be unity involves no loss of generality; it is consistent with the scaling of θ and ζ).

In the ensuing discussion, the (downstream) direction of increasing η shall often be referred to as north and the (cross-stream) direction of increasing ξ as east; however, if the western coastal orientation is not north–south, all results that follow will be valid, provided the (properly scaled) downstream variation of Coriolis parameter is used for β^* in numerical computations.

2.1. *Constant potential vorticity (CPV), first-order solution*

For this choice of P, equation (1.37) yields $\zeta_0 = \theta$ where the constant of integration is eliminated by taking $b_0 = 0$ and $h_0 = 1$. Equation (1.38) then becomes

$$\Pi_{1\xi\xi} + \Pi_{1\theta\theta} = -\beta^*, \quad (2.1)$$

with boundary conditions (1.39)–(1.42) to be satisfied. The substitution,

$$\Pi_1(\xi,\theta) = \sum_{n=1}^{\infty} A_n e^{-\lambda_n \xi}\phi_n(\theta) + \Pi_1^{\infty}(\theta), \tag{2.2}$$

leads to the equations,

$$\Pi_1^{\infty\prime\prime}(\theta) = -\beta^*, \tag{2.3}$$

$$K_0(\Pi_1^{\infty\prime}(0)+R_1) - \Pi_1^{\infty}(0) = K_1\Pi_1^{\infty\prime}(1) - \Pi_1^{\infty}(1) = 0, \tag{2.4}$$

and

$$\phi_n''(\theta) + \lambda_n^2\phi_n(\theta) = 0, \tag{2.5}$$

$$K_0\phi_n'(0) - \phi_n(0) = K_1\phi_n'(1) - \phi_n(1) = 0. \tag{2.6}$$

Note that (2.5) and (2.6) form a Sturm–Liouville (S–L) system. The solutions to the above are:

$$\Pi_1^{\infty} = -\tfrac{1}{2}\beta^*\theta^2 + C\theta + D, \tag{2.7}$$

$$\phi_n = \cos\lambda_n\theta + \gamma_n \sin\lambda_n\theta, \tag{2.8}$$

where

$$C = \frac{1}{\Delta_0}[K_0R_1 + \beta^*(K_1 - \tfrac{1}{2})], \tag{2.9}$$

$$D = K_0(C+R_1), \tag{2.10}$$

$$\gamma_n = \frac{1}{K_0\lambda_n}, \tag{2.11}$$

and $\Delta_0 \equiv K_1 - K_0 - 1$. The λ_m satisfy the equation

$$\tan\lambda_n = \frac{(K_1-K_0)\lambda_n}{1+K_0K_1\lambda_n^2}. \tag{2.12}$$

Now, inasmuch as λ_n^2 is the eigenvalue of an S–L system, it must be a real number; hence, λ_n is either a purely real number (consistent with a boundary-layer solution) or a purely imaginary number (inconsistent with a boundary-layer solution). Thus, it is necessary to seek restrictions on (K_0, K_1) so that (2.12) will be satisfied only by real λ_n or, equivalently, that the equation

$$\tanh\lambda_e = \frac{(K_1-K_0)\lambda_e}{1-K_0K_1\lambda_e^2}, \tag{2.13}$$

has no real solutions (see figure 1). As shown in IC, this constraint limits the allowed domain in (K_0, K_1)-space to one of three regions:

(1) $K_1 - 1 > K_0 \geqslant 0$,

(2) $0 \geqslant K_1 > K_0 + 1$,

(3) $K_0 \geqslant 0 \geqslant K_1$.

This result is shown in figure 2. (Spiegel (1966) has shown that it holds, not only for constant potential vorticity (CPV), but for any $P = P_0(\theta) > 0$, $P_{N>0} = 0$.) The physical meaning of the restrictions on (K_0, K_1) is that they select the classes

of geostrophic drift from the ocean's interior that are consistent with formation of an inertial boundary current. Specifically,

$$u_0^\infty(\theta) = -\Pi_1^\infty$$
$$= \tfrac{1}{2}\beta^*\theta^2 - \frac{1}{\Delta_0}[\beta^*(K_1-\tfrac{1}{2})+R_1K_0]\theta - \frac{K_0}{\Delta_0}[\beta^*(K_1-\tfrac{1}{2})+R_1(K_1-1)], \quad (2.14)$$

$$u_0^\infty(0) = -\frac{K_0}{\Delta_0}[\beta^*(K_1-\tfrac{1}{2})+R_1(K_1-1)], \quad (2.15)$$

$$u_0^\infty(1) = -\frac{K_1}{\Delta_0}[\beta^*(K_0+\tfrac{1}{2})+R_1K_0]. \quad (2.16)$$

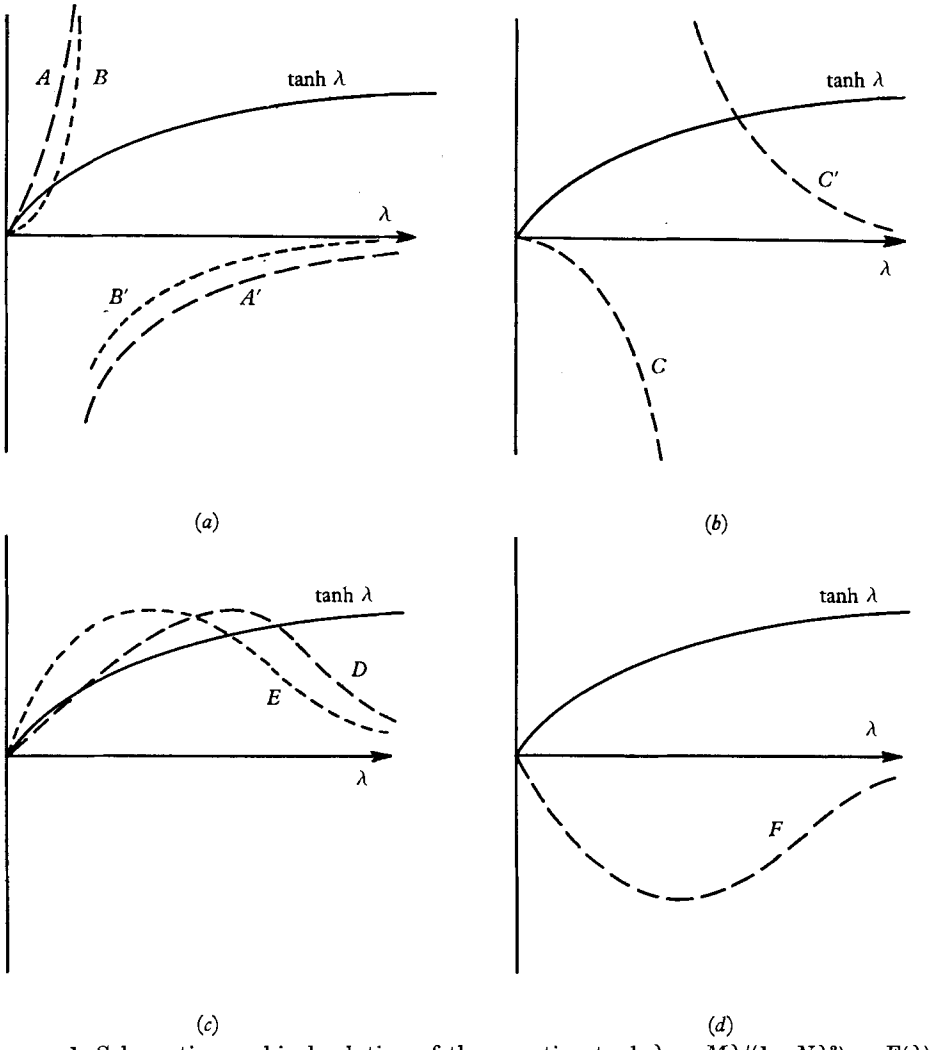

FIGURE 1. Schematic graphical solution of the equation $\tanh\lambda = M\lambda/(1-N\lambda^2) \equiv F(\lambda)$. In (*a*), $M > 0$ and $N > 0$. Curve A, A' is drawn for $F'(0) = M < 1$ and there is no non-zero solution. Curve B, B' is drawn for $M > 1$ and gives one non-zero solution. In (*b*), $M < 0$, $N > 0$ and there is always a non-zero solution. In (*c*), $M > 0$, $N < 0$ and if $F_{\max} \geqslant 1$ (as is the case for $M = K_1 - K_0$, $N = K_0K_1$), there will be one non-zero solution for $M > 1$ (curve E) and two for $M < 1$ (curve D). In (*d*), $M < 0$, $N < 0$ and there are no non-zero solutions.

For a flat bottom ($R_1 = 0$),

$$\frac{1}{\beta^*} u_0^\infty(0) = -\frac{K_0(K_1-\frac{1}{2})}{\Delta_0}, \quad \frac{1}{\beta^*} u_0^\infty(1) = -\frac{K_1(K_0+\frac{1}{2})}{\Delta_0}. \tag{2.17}$$

In region (1): $K_0 \geqslant 0, K_1 > 0, K_0+\frac{1}{2} > 0, K_1-\frac{1}{2} > 0, \Delta_0 > 0.$

In region (2): $K_0 < 0, K_1 \leqslant 0, K_0+\frac{1}{2} < 0, K_1-\frac{1}{2} < 0, \Delta_0 > 0.$

In region (3): $K_0 \geqslant 0, K_1 \leqslant 0, K_0+\frac{1}{2} > 0, K_1-\frac{1}{2} < 0, \Delta_0 < 0.$

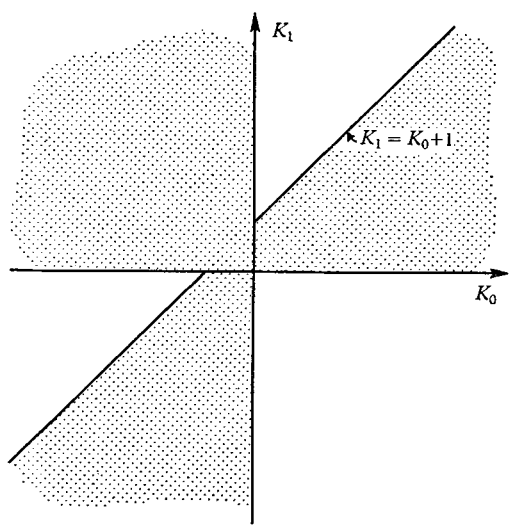

FIGURE 2. The (K_0, K_1)-plane showing the (unshaded) regions consistent with boundary current existence for constant potential vorticity, or more generally for any $P = P_0(\theta)$ (after Robinson, 1965*a*, figure 1).

Thus, it is clear that in all three permitted régimes, both $u_0^\infty(0)$ and $u_0^\infty(1)$ are negative; by virtue of (1.26) and (2.3), $u_0^{\infty\prime\prime}(\theta) > 0$, from which it follows that *for a flat bottom*, $u_0^\infty \leqslant 0$; i.e. the geostrophic drift must be westward at all levels, except that it may vanish at $\theta = 0$ or 1 if K_0 or K_1 is zero. From (2.4), it appears that one could also obtain vanishing $u_0^\infty(0)$ or $u_0^\infty(1)$ by requiring $\zeta_1^\infty(0)$ or $\zeta_1^\infty(1)$, respectively, to vanish, i.e. by having the lower or upper surface of the geostrophic interior be isothermal. However, from (2.7) and (2.4), or equivalently from (2.17), it is seen that imposing these conditions forces the choice $K_1 = \frac{1}{2}$ or $K_0 = -\frac{1}{2}$, respectively, and these values are in the forbidden region.

For $R_1 \neq 0$, these restrictions need not hold. Note that

$$\frac{\partial u_0^\infty}{\partial R_1} = -\frac{K_0}{\Delta_0}(\theta+K_1-1) \leqslant 0 \quad \text{for allowed } (K_0, K_1). \tag{2.18}$$

Hence, for fixed K_0, K_1 and θ, one can always find a (negative) value of R_1 for which u_0^∞ vanishes; steeper negative slopes will be associated with positive u_0^∞

(eastward flow). In particular, $u_0^\infty(0)$ or $u_0^\infty(1)$ can be made to vanish in two different ways. The first is by taking K_0 or K_1 to be zero, independent of the value of R_1. This will result in u_0 (and thus v_1) vanishing for all ξ at the surface in question. The second is by choosing R_1 so that the asymptotic bottom or top surface is isothermal. Here, the horizontal velocity components will, in general, be nonzero at the bottom or top within the boundary layer. These values of R_1 are denoted by R_1^0 and R_1^1, respectively:

$$u_0^\infty(0, R_1^0) = R_1^0 - \zeta_1^\infty(0, R_1^0) = u_0^\infty(1, R_1^1) = \zeta_1^\infty(1, R_1^1) = 0.$$

More negative values of R_1 will support eastward geostrophic drift at the bottom or top, respectively.

With the help of (1.66) and (1.67), it can readily be shown that for permitted (K_0, K_1),

$$R_1^1 = \beta^* \left(\frac{K_0 + \frac{1}{2}}{K_0}\right) \leqslant R_1^0 = -\beta^* \left(\frac{K_1 - \frac{1}{2}}{K_1 - 1}\right) < 0. \tag{2.19}$$

This indicates that for given (K_0, K_1), if R_1 is steadily decreased from zero, positive u_0^∞ will first appear at the lower boundary of the fluid. Also, the gentlest negative slope that can support eastward drift is R_1 just less than $-\frac{1}{2}\beta^*$ which occurs for $K_1 \to 0$; this corresponds to vanishing surface cross-stream flow. Note also that the curvature $u_0^{\infty\prime\prime}(\theta) = \beta^*$ is positive always.

The expression for the asymptotic transport is

$$U_0^\infty \equiv \int_0^1 u_0^\infty \, d\zeta_0 = \int_0^1 u_0^\infty \, \zeta_{0\theta} \, d\theta:$$

$$\begin{aligned} U_0^\infty &= \tfrac{1}{6}\beta^* - \tfrac{1}{2}C - D \\ &= \frac{1}{\Delta_0}\{\beta^*[\tfrac{1}{6}\Delta_0 - (K_1 - \tfrac{1}{2})(K_0 + \tfrac{1}{2})] - R_1 K_0 (K_1 - \tfrac{1}{2})\}. \end{aligned} \tag{2.20}$$

It is readily shown that for $R_1 = 0$, $U_0^\infty < 0$; the critical value of slope at which the transport changes sign is

$$R_1^T = \beta^*[\tfrac{1}{2} - 2(K_1 - K_0) - 6K_0 K_1]/[6K_0(K_1 - \tfrac{1}{2})] < 0, \tag{2.21}$$

and for $R_1 < R_1^T$, the boundary current will have a net outflow into the ocean's interior.

To complete the first-order solution, it is necessary to evaluate the A_n. These are determined by satisfying the boundary condition at $\xi = 0$ (equation (1.39)),

$$\Sigma A_n \phi_n(\theta) = -\Pi_1^\infty(\theta). \tag{2.22}$$

The function Π_1^∞ may be expanded in terms of the complete orthogonal set of functions $\{\phi_n\}$, the values of the expansion coefficients thus obtained for this example and those to follow are given by Spiegel (1966). The constant potential vorticity jet, to first order, is now completely specified:

$$\Pi_1(\xi, \theta) = \Sigma A_n \, e^{-\lambda_n \xi}[\cos \lambda_n \theta + \gamma_n \sin \lambda_n \theta] - \tfrac{1}{2}\beta^* \theta^2 + C\theta + D. \tag{2.23}$$

The other fields of interest are immediately obtainable from Π_1. In particular:

$$v_1(\xi,\eta) = -\Sigma\lambda_n A_n e^{-\lambda_n\xi}[\cos\lambda_n\theta+\gamma_n\sin\lambda_n\theta], \tag{2.24}$$

and

$$\zeta_1(\xi,\theta) = \Sigma\lambda_n A_n e^{-\lambda_n\xi}[\sin\lambda_n\theta-\gamma_n\cos\lambda_n\theta]+\beta^*\theta-C, \tag{2.25}$$

the last giving the first-order downstream slope of the isotherm heights.

2.2. *Constant potential vorticity, second-order solution*

Here, the appropriate form of (1.36) is

$$\Pi_{2\xi\xi}+\Pi_{2\theta\theta} = 2\beta^*\Pi_{1\xi\xi}, \tag{2.26}$$

where boundary conditions (1.44)–(1.47) apply. The detailed, explicit solution to this problem is found in Spiegel (1966). Briefly, substitution (1.48) is made, and the resultant $\hat{\Pi}$-equation is of the form

$$\hat{\Pi}_{\xi\xi}+\hat{\Pi}_{\theta\theta} = \Sigma C^{(m)}(\xi)\,\phi_m(\theta)+C_1(\xi)\,\theta+C_2(\xi), \tag{2.27}$$

with boundary conditions (1.50) and (1.51). Note that the right-hand side of (2.26) vanishes as $\xi\to\infty$. Since the $\phi_n(\theta)$ satisfy the same homogeneous part of the conditions on $\hat{\Pi}$, it is useful to make the expansion

$$\hat{\Pi}(\xi,\theta) = \sum_n \chi_n(\xi)\,\phi_n(\theta)+G\theta+H. \tag{2.28}$$

With the help of (1.50) and (1.51), it is easy to evaluate G and H, and after the right-hand side of (2.26) is expanded in terms of the ϕ_n, an equation for $\chi_n(\xi)$ is obtained of the form

$$\chi_n''-\lambda_n^2\chi_n = C^{(n)}(\xi)+\sum_m C_{nm}\exp\{-\lambda_m\xi\}+\sum\sum_{ml} C_{nml}\exp\{-(\lambda_m+\lambda_l)\xi\}. \tag{2.29}$$

The solution having the proper exponential decay at infinity is of the form

$$\chi_n(\xi) = [E_n+D_n\xi]\exp\{-\lambda_n\xi\}+\sum_{m\neq n} D_{nm}\exp\{-\lambda_m\xi\} +\sum\sum_{ml} D_{nml}\exp\{-(\lambda_m+\lambda_l)\xi\}, \tag{2.30}$$

where the D_n, D_{nm} and D_{nml} are known, and the E_n are determined by insisting that u_1 vanish at $\xi=0$; since Π_1 vanishes there already, it follows from (1.27) that the condition is

$$\Pi_2 = \Pi_{1\xi}^2 \quad \text{at} \quad \xi=0. \tag{2.31}$$

A straightforward but laborious calculation leads to an explicit solution of the second-order problem.

It should be noted that, from (1.38), (1.41), (1.42), (1.46) and (1.47), the amplitude of Π_1 is given by β^*, R_1 and R_2 as well as by K_0, K_1, L_0 and L_1. In particular, for a flat-bottomed ocean, Π_1 is proportional to β^* and Π_2 to β^{*2}. Thus, if the $K_{0,1}$ and $L_{0,1}$ dependences lead to order unity terms, the first-order solution will be a good approximation, provided $\eta < 1/\beta^*$. From the discussion of the η-scaling, it is seen that the physical co-ordinate condition is $y < f/\beta \equiv L_\beta$. Hence, although a 'thermal wind' scale length $(\Delta\rho g h/\rho_0 f_0 U_0)$ is important in

fixing the amplitudes of the solution, the physical length involved in the convergence of the downstream expansion is L_β, the natural length scale associated with df/dy. Of course, the existence of bottom topography introduces other natural geometrical length scales into the problem, and they serve to limit further the range in η for which the first-order solution is a good approximation.

Also, note that while K_0 and K_1 are of crucial importance in insuring the boundary-layer character of the flow to first order, L_0 and L_1 apparently have no corresponding role in determining the nature of the second-order fields, whose boundary-layer form is guaranteed by the reality of the λ_n^2. This could have been anticipated, since the same operator

$$\mathscr{L} \equiv \frac{\partial^2}{\partial \xi^2} + P_0 \frac{\partial^2}{\partial \theta^2} - \frac{P_I}{P_0^2}$$

and the same constants K_0, K_1 appear in the equations and boundary conditions for Π_1 and Π_2, and the right-hand side of the Π_2 equation is a function of Π_1. Hence, once K_0 and K_1 are selected so that Π_1 has an exponentially decaying ξ-dependence, the boundary conditions permit an expansion of Π_2 in the first-order eigenfunctions $\phi_n(\theta)$; the resulting ξ-equation will then have properly decaying homogeneous and particular solutions. This reasoning applies to the higher-order equations as well, the form of which is

$$\mathscr{L}(\Pi_n) = f(\Pi_1, \Pi_2, \ldots, \Pi_{n-1}).$$

Therefore, the existence of the boundary current to all orders depends upon the proper choice of K_0 and K_1, or equivalently, appropriate values of u_0^∞ and ζ_1^∞. In particular, for flat bottom, a constraint is found on the sign of u^∞ but not on its downstream variation.

However, it would be premature to assert that the values of L_0 and L_1 are totally unrestricted. The term proportional to $\xi e^{-\lambda_1 \xi}$ (see equation (2.30)) that ultimately appears in the Π_2-solution indicates a lack of uniform convergence of the η-expansion. It is a simple matter to find a functional dependence $L_1 = f_1(L_0)$ such that the term proportional to $e^{-\lambda_1 \xi}$ is absent from the right-hand side of (2.29); this will remove the offensive term from the Π_2-solution corresponding to this particular flow. Also, using a modified Lighthill (1949) technique, one can find a second relation $L_1 = f_2(L_0)$ corresponding to another flow field, such that the $\xi e^{-\lambda_1 \xi}$ term does not appear in Π_2; here, Π_1 is modified by having its ξ-dependent part multiplied by a factor $\exp(-\frac{1}{2}\beta\eta\lambda_1\xi)$, indicating a downstream narrowing of the boundary current. So it would seem that a more complete investigation of the convergence problem might well result in limiting the values of L_0 and L_1, and hence limiting the classes of u_1^∞, consistent with maintaining a boundary current. Inasmuch as this task remains to be done even for the simplest CPV case, the detailed second-order solutions for the other potential vorticity forms will not be given here (these are easy enough to derive if need be). It seems reasonable, however, that the first-order solutions obtained, which boundary layer properly and join smoothly with the interior fields, will at most be in need of a small quantitative downstream modification. This is certainly true in the two instances mentioned above.

Hence, the investigation of the second-order problem indicates that, for oceanic flows whose downstream variation is slow enough so that this expansion technique can provide an adequate description, the question of the existence of a boundary current is resolved by examining the first-order solution. No further fundamental constraints on the driving interior fields are obtained by going to second (or higher) order. To put it another way, within the region of validity of the expansion, existence is found to depend upon the local values of u^∞ and $\partial\zeta^\infty/\partial\eta$, and not on any higher-order derivatives.

Finally, note the physically pleasing result that the bottom slope parameter R_1 always appears multiplied by K_0 in the first-order solution, although not in the second-order solution. Thus, to lowest order, the slope R_1 will not be 'felt' by an incoming baroclinic u-field ($u_0(0) = K_0 = 0$); it will, however, influence the higher-order solutions.

2.3. *First-order solution for* $P = 1 - \alpha^2\psi$

This choice of the potential vorticity function maintains the linear zero-order stratification inherent in the CPV model, but is capable of describing a wider variety of asymptotic zero-order u-fields and downstream density gradients. The first-order Π-equation becomes

$$\Pi_{1\xi\xi} + \Pi_{1\theta\theta} + \alpha^2\Pi_1 = -\beta^*, \tag{2.32}$$

with boundary conditions (1.39)–(1.42); the choice $b_0 = 0$ and $s_0 = 1$ may be consistently retained. The substitution,

$$\Pi_1(\xi,\theta) = \sum_n A_n e^{-k_n\xi}\phi_n(\theta) + \Pi_1^\infty(\theta), \tag{2.33}$$

is made in (2.39), and there results the equations:

$$\Pi_1^{\infty\prime\prime} + \alpha^2\Pi_1^\infty = -\beta^*, \tag{2.34}$$

$$\phi_n'' + \lambda_n^2\phi_n = 0, \quad \lambda_n^2 \equiv k_n^2 + \alpha^2, \tag{2.35}$$

$$\begin{aligned} K_0(\Pi_1^{\infty\prime}(0) + R_1) - \Pi_1^\infty(0) &= K_1\Pi_1^{\infty\prime}(1) - \Pi_1^\infty(1) \\ &= K_0\phi_n'(0) - \phi_n(0) = K_1\phi_n'(1) - \phi_n(1) = 0. \end{aligned} \tag{2.36}$$

The solution is readily found to be:

$$\Pi_1^\infty = -\frac{\beta^*}{\alpha^2} + C\cos\alpha\theta + D\sin\alpha\theta, \tag{2.37}$$

$$\phi_n = \cos\lambda_n\theta + \gamma_n\sin\lambda_n\theta, \tag{2.38}$$

where
$$D = \frac{1}{\Delta_-}\left[\frac{\beta^*}{\alpha^2}(K_1\alpha\sin\alpha + \cos\alpha - 1) + R_1K_0(\cos\alpha + K_1\alpha\sin\alpha)\right], \tag{2.39}$$

$$C = \frac{\beta^*}{\alpha^2} + K_0(R_1 + \alpha D), \tag{2.40}$$

$$\Delta_- \equiv (K_1 - K_0)\alpha\cos\alpha - (1 + K_0K_1\alpha^2)\sin\alpha, \tag{2.41}$$

$$\gamma_n = \frac{1}{K_0\lambda_n}, \tag{2.42}$$

and the λ_n satisfy the relation

$$\tan\lambda_n = \frac{(K_1 - K_0)\lambda_n}{1 + K_0 K_1 \lambda_n^2}. \tag{2.43}$$

Now, for a boundary current, the k_n must all be real; and so the requirement on the λ_n becomes $\lambda_n^2 > \alpha^2$ for all n, a more stringent condition than in the previous case. Thus, for $\alpha^2 > 0$, it is clear that the permitted region of (K_0, K_1)-space will be reduced from its CPV extent. This is shown in figure 3 which is drawn for the case $\alpha^2 = 1$. Use is made of (2.43) solved for K_1:

$$K_1 = \frac{K_0 + (1/\lambda)\tan\lambda}{1 - K_0\lambda\tan\lambda}.$$

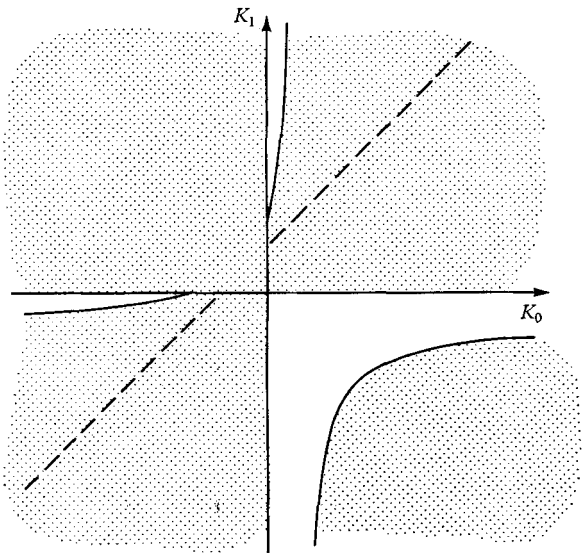

FIGURE 3. The (K_0, K_1)-plane showing the (unshaded) regions consistent with boundary current existence for $P_0 = 1$, $P_I = -\alpha^2$. The hyperbolic curve satisfies the equation $K_1 = (K_0 + \tan 1)/(1 - K_0 \tan 1)$. The dashed line $K_1 = K_0 + 1$ is included for comparison with figure 2.

By varying λ, one obtains a family of hyperbolas in K_0 and K_1; the choice $\lambda^2 = \alpha^2$ results in the hyperbola that, with the axes, serves as the limiting boundaries of the allowed domain. For $\alpha^2 \geqslant \pi^2$, the entire (K_0, K_1)-plane is forbidden; i.e. no boundary-layer solutions can exist.

An investigation of the correspondingly allowed asymptotic fields once again shows that with a flat bottom, only geostrophic drift that is westward at all levels (except that it may vanish at $\theta = 0$ or 1) is consistent with achieving a coastal boundary current. In detail,

$$\begin{aligned} u_0^{\infty}(\theta) = \frac{1}{\Delta_-}\Bigg\{\beta^*\Bigg[&(K_1 - K_0)\frac{\cos\alpha}{\alpha} - \left(\frac{1}{\alpha^2} + K_0 K_1\right)\sin\alpha \\ &+ \left(\frac{\sin\alpha}{\alpha^2} + \frac{K_0 - K_1\cos\alpha}{\alpha}\right)\cos\alpha\theta + \left(\frac{1-\cos\alpha}{\alpha^2} - \frac{K_1\sin\alpha}{\alpha}\right)\sin\alpha\theta\Bigg] \\ &+ R_1 K_0[(\sin\alpha - K_1\alpha\cos\alpha)\cos\alpha\theta - (\cos\alpha + K_1\alpha\sin\alpha)\sin\alpha\theta]\Bigg\}. \end{aligned} \tag{2.44}$$

A careful determination of the properties of this expression as K_0 and K_1 are varied indicates also that $\partial u_0^\infty/\partial R_1 < 0$ and $u_{0\theta\theta}^{\infty\prime\prime}|_{R_1=0} > 0$ always in the region of interest. The bottom velocity will vanish for a slope

$$R_1^0 = -\frac{\beta^*}{\alpha}\left[\frac{K_1\alpha\sin\alpha+\cos\alpha-1}{K_1\alpha\cos\alpha-\sin\alpha}\right]; \tag{2.45}$$

for $R_1 < R_1^0$, $u_0^\infty(0)$ will be positive. At the top, the slope for vanishing u_0^∞ is

$$R_1^1 = -\frac{\beta^*}{\alpha^2 K_0}[K_0\alpha\sin\alpha-\cos\alpha+1]. \tag{2.46}$$

R_1^0 and R_1^1 are both negative for allowed K_0 and K_1; the smallest negative value for R_1^0 occurs for $K_1 = 0$.

The expression for the transport is easily derived from (2.44):

$$U_0^\infty = \frac{1}{\Delta_-}\left\{\beta^*\left[\frac{2}{\alpha^3}(1-\cos\alpha)-\frac{\sin\alpha}{\alpha^2}(K_1-K_0+1)+\frac{\cos\alpha}{\alpha}(K_1-K_0)-K_1K_0\sin\alpha\right]\right.$$
$$\left.+\frac{R_1K_0}{\alpha}[1-\cos\alpha-K_1\alpha\sin\alpha]\right\}; \tag{2.47}$$

this is negative for $R_1 = 0$.

2.4. *First-order solution for* $P = 1+\alpha^2\psi$

Here, the first-order Π-equation is

$$\Pi_{1\xi\xi}+\Pi_{1\theta\theta}-\alpha^2\Pi_1 = -\beta^*, \tag{2.48}$$

and using the usual separation technique, one can write the solution in the form:

$$\Pi_1(\xi,\theta) = \sum_n A_n e^{-k_n\xi}(\cos\lambda_n\theta+\gamma_n\sin\lambda_n\theta)+\frac{\beta^*}{\alpha^2}+C\cosh\alpha\theta+D\sinh\alpha\theta, \tag{2.49}$$

where

$$\lambda_n^2 = k_n^2-\alpha^2, \tag{2.50}$$

$$\tan\lambda_n = \frac{(K_1-K_0)\lambda_n}{1+K_0K_1\lambda_n^2}. \tag{2.51}$$

The requirement of real k_n no longer imposes the restriction of real λ_n. Thus, eigenvalues λ_m^* that satisfy

$$\tanh\lambda_m^* = \frac{(K_1-K_0)\lambda_m^*}{1-K_0K_1\lambda_m^{*2}}, \tag{2.52}$$

$$\lambda_m^{*2} = \alpha^2-k_m^2, \tag{2.53}$$

will be perfectly consistent with a boundary current, provided they also satisfy the inequality $\lambda_m^{*2} < \alpha^2$. It is easy to see graphically that (2.53) can have, at most, two non-zero solutions. Also, for the case $K_1 = K_0+1$,

$$\phi_0 = \theta+K_0 \tag{2.54}$$

is a relevant eigenfunction, belonging to the eigenvalue $\lambda_0 = 0$ (the corresponding $k_0 = \alpha$). Hence, the solution may be rewritten in the form:

$$\Pi_1(\xi,\theta) = N_0 A_0 e^{-\alpha\xi}\phi_0(\theta) + \sum_{m=1}^{N_h} A_m^* e^{-k_m\xi}\phi_m^*(\theta) + \sum_{n=N_h+1}^{\infty} A_n e^{-k_n\xi}\phi_n(\theta) + \frac{\beta^*}{\alpha^2} + C\cosh\alpha\theta + D\sinh\alpha\theta, \quad (2.55)$$

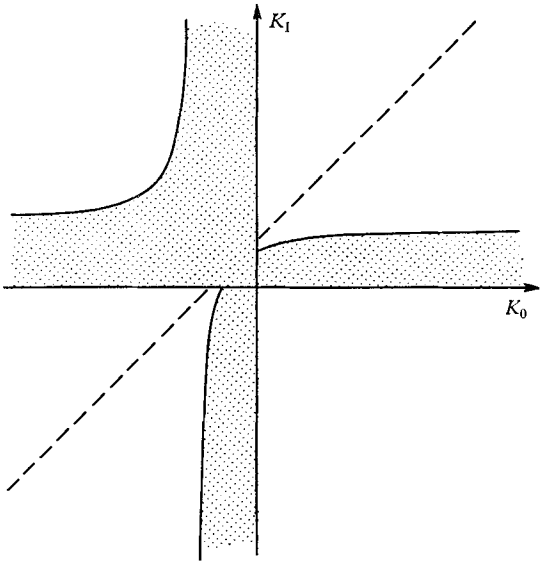

FIGURE 4. The (K_0, K_1)-plane showing the (unshaded) regions consistent with boundary current existence for $P_0 = 1, P_I = \alpha^2$. In the permitted region between the hyperbolic curve $K_1 = (K_0 + \tanh 1)/(1 + K_0 \tanh 1)$ and the dashed line $K_0 = K_1 + 1$, hyperbolic θ-eigenfunctions are required.

where N_0 is either 0 or 1, N_h is 0, 1 or 2, and

$$\phi_n = \cos\lambda_n\theta + \gamma_n \sin\lambda_n\theta, \quad (2.56)$$

$$\phi_m^* = \cosh\lambda_m^*\theta + \gamma_m^* \sinh\lambda_m^*\theta, \quad (2.57)$$

$$\gamma_n = \frac{1}{K_0\lambda_n}, \quad \gamma_m^* = \frac{1}{K_0\lambda_m^*}, \quad (2.58)$$

$$D = \frac{1}{\Delta_+}\left[\frac{\beta^*}{\alpha^2}(1 - \cosh\alpha + K_1\alpha\sinh\alpha) + R_1K_0(\cosh\alpha - \alpha K_0\sinh\alpha)\right], \quad (2.59)$$

$$C = -\frac{\beta^*}{\alpha^2} + K_0(\alpha D + R_1), \quad (2.60)$$

$$\Delta_+ \equiv (K_1 - K_0)\alpha\cosh\alpha + (\alpha^2K_0K_1 - 1)\sinh\alpha. \quad (2.61)$$

The acceptability of hyperbolic eigenfunctions is paralleled by an increase in the permitted region of K_0, K_1 space. Figure 4 is drawn for the case $\alpha^2 = 1$. The area now permitted, which was forbidden for CPV, corresponds to solutions with $N_h \neq 0$. For $\alpha^2 \to \infty$, the entire (K_0, K_1)-plane 'opens up': any values of these parameters will be descriptive of coastal boundary currents. However, careful

inspection of the resultant asymptotic fields shows that, in all cases, the familiar restrictions obtain in the range $0 < \theta < 1$:

$$u_0^\infty(\theta) = \frac{1}{\Delta_+}\left\{\beta^*\left[\left(\frac{1}{\alpha^2} - K_0K_1\right)\sinh\alpha - (K_1 - K_0)\frac{\cosh\alpha}{\alpha}\right.\right.$$
$$+\left(\frac{K_1}{\alpha}\cosh\alpha - \frac{K_0}{\alpha} - \frac{\sinh\alpha}{\alpha^2}\right)\cosh\alpha\theta + \left(\frac{\cosh\alpha - 1}{\alpha^2} - \frac{K_1}{\alpha}\sinh\alpha\right)\sinh\alpha\theta\Big]$$
$$+R_1K_0[(\sinh\alpha - K_1\alpha\cosh\alpha)\cosh\alpha\theta$$
$$\left.+(\alpha K_1\sinh\alpha - \cosh\alpha)\sinh\alpha\theta]\right\}$$
$$< 0; \quad \text{for } R_1 = 0; \tag{2.62}$$
$$\frac{\partial u_0^\infty}{\partial R_1} < 0, \quad u_{0\theta\theta}^\infty|_{R_1=0} > 0,$$
$$R_1^0 = -\frac{\beta^*}{\alpha}\left[\frac{K_1\alpha\sinh\alpha - \cosh\alpha + 1}{K_1\alpha\cosh\alpha - \sinh\alpha}\right] < 0, \tag{2.63}$$

and has its smallest negative value for $K_1 = 0$,

$$R_1^1 = -\frac{\beta^*}{\alpha^2K_0}[K_0\alpha\sinh\alpha + \cosh\alpha - 1], \tag{2.64}$$

$$U_0^\infty = \frac{1}{\Delta_+}\left\{\beta^*\left[\frac{2}{\alpha^3}(1-\cosh\alpha) + \frac{\sinh\alpha}{\alpha^2}(K_1 - K_0 + 1)\right.\right.$$
$$\left.-\frac{\cosh\alpha}{\alpha}(K_1 - K_0) - K_0K_1\sinh\alpha\right] + \frac{R_1K_0}{\alpha}(\cosh\alpha - 1 - K_1\alpha\sinh\alpha)\Big\}$$
$$< 0 \quad \text{for } R_1 = 0. \tag{2.65}$$

The quantities R_1^0, R_1^1 and U_0^∞ have their usual definitions.

Thus while a potential vorticity function with a linear ψ-dependence ($P = 1 \pm \alpha^2\psi$) is descriptive of a much wider class of asymptotic fields consistent with boundary current formation than the constant potential vorticity case (to which the results properly reduce in the limit $\alpha \to 0$), the westward drift condition at all levels for a flat bottom is not relaxed. Eastward drift is possible only with a bottom that deepens sufficiently rapidly in the downstream direction, the value of such a slope being a function of the other parameters of the system.

To see this more clearly, note that the asymptotic form of (1.38) can be written:

$$P_0\Pi_{1\theta\theta}^\infty - \frac{P_I}{P_0^2}\Pi_1^\infty = -\beta^*, \tag{2.66}$$

or equivalently,
$$u_{0\theta\theta}^\infty = \zeta_{1\theta}^\infty = \frac{1}{P_0}\left[\frac{P_I}{P_0^2}u_0^\infty + \beta^*\right]. \tag{2.67}$$

Recall $P_0 > 0$ for stable stratification. In the appendix, it is shown that for $R_1 = 0$, $\Pi_1^\infty > 0$, $0 < \theta < 1$, always; hence, for $P_I < 0$, $\Pi_{1\theta\theta}^\infty < 0$ for flat bottom and it will remain negative until the slope is adjusted to yield negative Π_1^∞ (i.e. $u_0^\infty > 0$). This means that positive u_0^∞ will first appear at the upper or lower surface; in the examples studied, it has always appeared first at the bottom. Recall that the slope at which $u_0^\infty(0)$ changes sign is that for which the asymptotic

bottom surface becomes an isotherm, i.e. for which $R_1^0 = \zeta_0^\infty(0, R_1^0)$. After a θ-integration of (2.67), this condition can be written

$$R_1^0 = \zeta_1^\infty(1) - \left[\beta^* + \int_0^1 \frac{P_I}{P_0^2} u_0^\infty \, d\zeta_0\right], \tag{2.68}$$

where the right-hand side is a function of R_1 and the relation $P_0^{-1} = \partial\zeta_0/\partial\theta$ has been used. On the assumption that u_0^∞ first changes sign at the bottom for all potential vorticities, then $u_0^\infty \leqslant 0$ in the range of integration of (2.68) and one can thus see a tendency for potential vorticities with $P_I(\theta) > 0$ (or 'mostly' positive, in the appropriate sense) to require a less negative bottom slope to achieve positive u_0^∞ than for $P_I = 0$, the reverse being true for $P_I < 0$. In particular, for the case of an isothermal upper surface ($\zeta_1^\infty(1) = 0$), it is evident that for

$$\begin{aligned} P &= 1 + \alpha^2\psi, \quad & R_1^0 &> -\beta^* \text{ (less steep)}, \\ P &= 1, & R_1^0 &= -\beta^*, \\ P &= 1 - \alpha^2\psi, & R_1^0 &< -\beta^* \text{ (steeper)}. \end{aligned}$$

In addition, an analysis of (2.53) and (2.76) shows that for $P = 1 + \alpha^2\psi$, the gentlest negative slope that can produce vanishing $u_0^\infty(0)$ goes from $-0{\cdot}5\beta^*$ for $\alpha \to 0$ to zero for $\alpha \to \infty$ (but $\Pi_1^\infty \to 0$ also in this limit, implying vanishingly small flow); whereas for $P = 1 - \alpha^2\psi$, the value varies from $-0{\cdot}5\beta^*$ for $\alpha \to 0$ to $-\infty$ for $\alpha \to \pi$. Also, it is seen from (2.67) that $u_{0\theta\theta}^\infty$ is greater for $P_I < 0$ than for $P_I > 0$ at $R_1 = R_1^0$; hence, there is a tendency for large (positive) curvature of u_0^∞ to be associated with steep (negative) R_1^0.

Unfortunately, it is hard to delve further into the mathematical formalism to gain a clearer insight into the physical processes that lead to the constraints we have discovered. Although the results for specific examples are everywhere consistent with the existence criteria for transport formulated by Greenspan (1962, 1963) and Pedlosky (1965), a simple expression of constraint based on the density space formulation has not yet been derived.

2.5. *First-order solution with thermocline structure*: $P = \theta^2/a$

In the examples considered above, the zero-order stratification has always been linear ($\zeta_0 = \theta$), owing to the constancy of P_0. The real ocean exhibits a thermocline behaviour, with steeper thermal gradients occurring near the top than at the bottom. To model this more realistically, it is necessary to allow P_0 to have a temperature dependence. For example, the choice $P_0 = \theta/d$ leads to a temperature field $\theta = e^{-(\zeta-1)/d}$ which decays by a factor $1/e$ from its surface value in a distance $d > 0$ below the surface; a proper choice of d will produce a realistic looking temperature profile. The resultant Π_1-equation may be solved without difficulty, yielding the result

$$\Pi_1 = \sum_n \exp\{-\sqrt{(d)}\lambda_n\xi\}\{2A_n\lambda_n\theta^{\frac{1}{2}}[J_1(2\lambda_n\theta^{\frac{1}{2}}) + \gamma_n Y_1(2\lambda_n\theta^{\frac{1}{2}})]\} - \frac{\beta^*}{d}[\theta\ln(C\theta) + D]. \tag{2.69}$$

However, the choice $P_0 = a^{-1}\theta^2$ is also capable of describing realistic temperature profiles, and since the mathematics involved in obtaining the eigenvalues and expansion coefficients is somewhat simpler, this is the form to be investigated. Thus, using (1.63), it follows that

$$\zeta_0 = c - a/\theta. \tag{2.70}$$

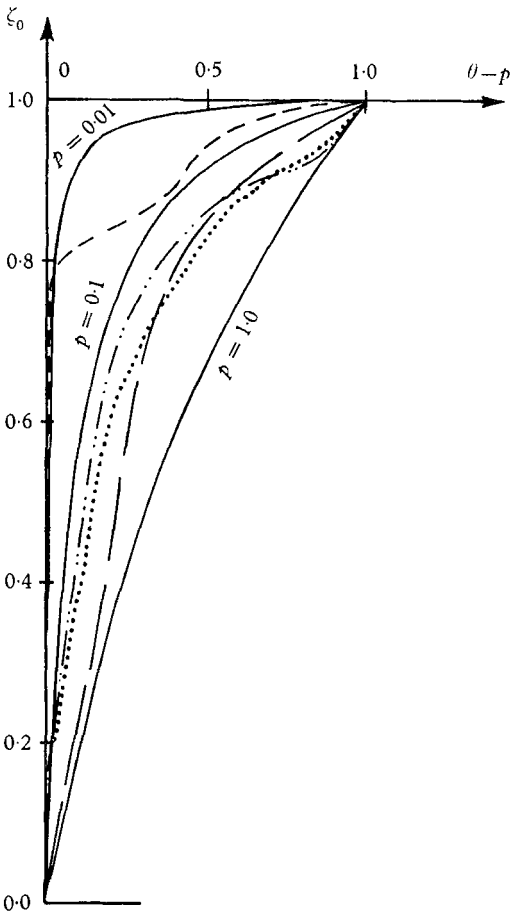

FIGURE 5. Asymptotic zero-order density profiles corresponding to $P = \theta^2/p(p+1)$ for indicated values of p, compared with suitably scaled oceanic density profiles calculated from data given by Iselin (1936), Fuglister (1960), and the Commonwealth Scientific and Industrial Research Organization, Australia (C.S.I.R.O. Aust., 1963). Oceanic density profiles: —··—··—, at seaward edge of Florida current off Cape Kennedy (Canaveral), 28°N., 79°W.; — —, at seaward edge of Florida current off Jacksonville, 30°N., 79°W.; ------, at seaward edge of the East Australia current off Brisbane, 27°S., 155°E.; – – – –, in the south-eastern North Atlantic (24°N., 72°W.) well beyond the seaward edge of the Florida current.

In this case, it is convenient to let $b_0 = p > 0$, $s_0 = q = p+1$. Then, with the choice $a = pq$, $c = q$, θ will go from p to q as ζ_0 varies from 0 to 1:

$$\zeta_0 = q(1 - p/\theta), \quad \text{or} \quad \theta = pq/(q - \zeta_0). \tag{2.71}$$

Figure 5 shows temperature or, more properly, density profiles for various values of p; these are compared with profiles calculated from temperature and salinity

measurements taken at several points seaward off the Florida and East Australia Currents. It is seen that judicious choices of p will provide qualitatively good approximations to the oceanic curves.

For this case, the Π_1-equation is

$$\Pi_{1\xi\xi}+\frac{\theta^2}{pq}\Pi_{1\theta\theta}=-\beta^*, \tag{2.72}$$

with boundary conditions (1.39)–(1.42) in effect. It is now useful to put

$$\Pi_1(\xi,\theta)=\sum_n A_n\exp\{-k_n(pq)^{-\frac{1}{2}}\xi\}\phi_n(\theta)+\Pi_1^\infty(\theta), \tag{2.73}$$

whence

$$\Pi_1^{\infty\prime\prime}=-pq\beta\theta^{-2}, \tag{2.74}$$

$$\phi_n''+\frac{k_n^2}{\theta^2}\phi_n=0, \tag{2.75}$$

and

$$\begin{aligned}K_0(\Pi_1^{\infty\prime}(p)+R_1)-\Pi_1^\infty(p)&=K_1\Pi_1^{\infty\prime}(q)-\Pi_1^\infty(q)\\&=K_0\phi_n'(p)-\phi_n(p)=K_1\phi_n'(q)-\phi_n(q)=0.\end{aligned} \tag{2.76}$$

The asymptotic solution is

$$\Pi_1^\infty=pq\beta^*[\ln\theta+C\theta+D], \tag{2.77}$$

where

$$C=\frac{1}{\Delta_0}\left[\frac{K_0}{p}-\frac{K_1}{q}+\ln\frac{q}{p}+\frac{R_1K_0}{pq\beta^*}\right], \tag{2.78}$$

and

$$D=\frac{K_1}{q}-\ln q+(K_1-q)C=\frac{K_0}{p}-\ln p+(K_0-p)C+\frac{R_1K_0}{pq\beta^*}. \tag{2.79}$$

The $\phi_n(\theta)$ have different forms, depending on whether the associated k_n^2 is greater than, equal to, or smaller than $\frac{1}{4}$. For $k_n^2>\frac{1}{4}$, we have

$$\phi_n=\theta^{\frac{1}{2}}[\cos(\lambda_n\ln\theta)+\gamma_n\sin(\lambda_n\ln\theta)], \tag{2.80}$$

where λ_n, which is defined by $\lambda_n^2\equiv k_n^2-\frac{1}{4}$, satisfies the eigenvalue equation,

$$\tan\left(\lambda_n\ln\frac{q}{p}\right)=\frac{(pK_1-qK_0)\lambda_n}{pq-\frac{1}{2}(pK_1+qK_0)+K_0K_1(\frac{1}{4}+\lambda_n^2)} \tag{2.81}$$

and

$$\gamma_n=\frac{(q-\frac{1}{2}K_1)\cos(\lambda_n\ln q)+K_1\lambda_n\sin(\lambda_n\ln q)}{(\frac{1}{2}K_1-q)\sin(\lambda_n\ln q)+K_1\lambda_n\cos(\lambda_n\ln q)}. \tag{2.82}$$

The eigenfunction,

$$\phi_0=\theta^{\frac{1}{2}}[1+\gamma_0\ln\theta], \tag{2.83}$$

which corresponds to the case $k_n^2=\frac{1}{4}$ is only a relevant solution if the relation,

$$K_1=\frac{2q\left[K_0\left(\ln\frac{q}{p}-2\right)-2p\ln\frac{q}{p}\right]}{K_0\ln\frac{q}{p}-2p\left(2+\ln\frac{q}{p}\right)}, \tag{2.84}$$

is satisfied. In that case,

$$\gamma_0=(2p-K_0)/[(2+\ln p)K_0-2p\ln p]. \tag{2.85}$$

For $0 < k_m^2 < \frac{1}{4}$, define $\lambda_m^{*2} \equiv \frac{1}{4} - k_m^2$. Note that the requirement of real k_m means that only values of $\lambda_m^{*2} < \frac{1}{4}$ are consistent with a boundary current. If the associated eigenfunctions are denoted by ϕ_m^*, then:

$$\phi_m^* = \theta^{\frac{1}{2}}[\cosh(\lambda_m^* \ln\theta) + \gamma_m^* \sinh(\lambda_m^* \ln\theta)], \tag{2.86}$$

$$\tanh\left(\lambda_m^* \ln\frac{q}{p}\right) = \frac{(pK_1 - qK_0)\lambda_m^*}{pq - \frac{1}{2}(pK_1 + qK_0) + K_0K_1(\frac{1}{4} - \lambda_m^{*2})}, \tag{2.87}$$

$$\gamma_m^* = \frac{(q - \frac{1}{2}K_1)\cosh(\lambda_m^* \ln q) - K_1\lambda_m^* \sinh(\lambda_m^* \ln q)}{(\frac{1}{2}K_1 - q)\sinh(\lambda_m^* \ln q) + K_1\lambda_m^* \cosh(\lambda_m^* \ln q)}. \tag{2.88}$$

Graphical analysis reveals that the eigenvalue equation (2.84) has no more than two non-zero solutions.

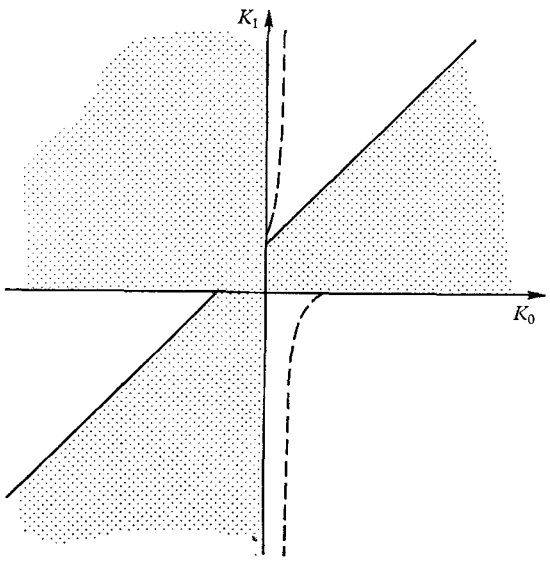

FIGURE 6. The (K_0, K_1)-plane showing the (unshaded) regions consistent with boundary-layer existence for $P = \theta^2/p(p+1)$. The dashed hyperbola gives the relation between K_0 and K_1 for $\lambda = 0$, and is drawn for $p = 0{\cdot}1$. In the permitted region between this curve and the K_1-axis, only eigenfunctions of the type given by (2.93) are required.

The condition on λ_m^{*2} defines an allowed region in (K_0, K_1)-space; this is shown in figure 6. As noted previously, the forbidden regions coincide with those found for the CPV case. In finding the diagonal boundary in the figure, the line $K_1 = K_0 + 1$, use has been made of the identity

$$\tanh(\tfrac{1}{2}\ln x) \equiv (x-1)/(x+1).$$

The portion of allowed (K_0, K_1)-space that requires only eigenfunctions of the type $\phi_n(\theta)$, $n \neq 0$, has been drawn for the case $p = 0{\cdot}1$.

Once more, it is found that for $R_1 = 0$, all permitted K_0, K_1 values lead to negative values of $u_0^\infty(\theta)$, $p < \theta < q$. A study of the explicit form of u_0^∞, namely,

$$u_0^\infty = -\frac{pq\beta^*}{\Delta_0}\left[\Delta_0\left(\ln\theta - \ln q + \frac{K_1}{q}\right) + \left(\frac{K_0}{p} - \frac{K_1}{q} + \ln\frac{q}{p}\right)(\theta - q + K_1)\right] - \frac{R_1K_0}{\Delta_0}[\theta - q + K_1], \tag{2.89}$$

reveals that the other familiar results obtain as well, thermocline or no:

$$\frac{\partial u_0^\infty}{\partial R_1} < 0, \quad u_{0\theta\theta}^\infty|_{R_1=0} > 0,$$

$$R_1^0 = \frac{pq\beta^*}{K_0(K_1-1)}\left[\Delta_0\left(\frac{K_1}{q}-\ln\frac{q}{p}\right)+(K_1-1)\left(\frac{K_0}{p}-\frac{K_1}{q}\right)\right] < 0, \tag{2.90}$$

$$R_1^1 = -\frac{pq\beta^*}{K_0K_1}\left[\Delta_0\frac{K_1}{q}+K_1\left(\frac{K_0}{p}-\frac{K_1}{q}+\ln\frac{q}{p}\right)\right] < 0, \tag{2.91}$$

where R_1^0 and R_1^1 are defined in the usual way.

In evaluating

$$U_0^\infty \equiv \int_0 u_0^\infty d\zeta_0,$$

one must take care to note that $\zeta_{0\theta} = 1/P_0 = pq\theta^{-2}$, and not unity as in the previous examples. Therefore,

$$\begin{aligned} U_0^\infty = pq\int_p^q u_0^\infty\theta^{-2}d\theta = \frac{pq\beta^*}{\Delta_0}\Bigg\{&\Delta_0\left[\frac{1}{q}(\ln q+1)-\frac{1}{p}(\ln p+1)\right] \\ &-\ln\frac{q}{p}\left(\frac{K_0}{p}-\frac{K_1}{q}+\ln\frac{q}{p}\right)-\frac{1}{pq}\left[\Delta_0\left(\frac{K_1}{q}-\ln q\right)+(K_1-q)\left(\frac{K_0}{p}-\frac{K_1}{q}+\ln\frac{q}{p}\right)\right]\Bigg\} \\ &-\frac{R_1K_0}{\Delta_0}\left\{\frac{K_1-q}{pq}-\ln\frac{q}{p}\right\}, \end{aligned} \tag{2.92}$$

and for $R_1 = 0$, $U_0^\infty < 0$.

It should be pointed out that in the foregoing analysis, the tacit assumption has been made that the three defined quantities Δ_0, Δ_+ and Δ_- were non-zero, or equivalently, (K_0, K_1) values were not chosen on the diagonal or hyperbolic boundaries of the allowed regions. If they are chosen on such a curve, then and only then must the θ-eigenfunction corresponding to the ξ-eigenvalue $k_0 = 0$ ($\lambda_0 = 0$ for CPV) be included in the complete set of eigenfunctions. This new eigenfunction will be a linear combination of the two terms multiplied by C and D in the expression for the corresponding Π_1^∞, and since it does not decay with ξ, will modify the field at ∞. If it is possible to choose (K_0, K_1) on the curve so that the amplitude of Π_1 remains finite, then the solution will not differ qualitatively from other solutions with (K_0, K_1) inside the permitted zones and the same constraints will be obeyed. It can be shown that it is impossible to so choose (K_0, K_1) for flat bottom in the examples studied above; for these cases, the appropriate 'Δ' is required to be non-zero.

In fact, it is readily shown that the case of constant Coriolis parameter ($\beta^* = 0$) with uniform depth imposes a $\Delta = 0$ relationship, and since the solution of the resulting homogeneous Π_1^∞ equation is of precisely the same form as the ξ-independent member of the set of Π_1 eigenfunctions, the system has the trivial solution $\Pi_1 = 0$. However, a non-trival solution can exist for $\beta^* = 0$, $R_1 \neq 0$ where it is possible to have $\Delta \neq 0$. Thus, a boundary current can exist in a uniformly rotating system, but only if the depth varies in the downstream direction. It must be emphasized that this conclusion holds only for the $v_0 = 0$ boundary

current. Free inertial currents (with $v_0 \neq 0$) in a uniformly rotating ocean have been discussed by Robinson & Niiler (1967), but the boundary current remains to be studied.

2.6. *The onshore countercurrent*

It has been seen that it is possible to have eastward geostrophic drift at any and all levels, provided the bottom deepens rapidly enough in the downstream direction. That is, $\Pi_1(\infty, \theta)$ can be negative under the right conditions and still be consistent with a boundary current. But it is also required that $\Pi_1(0, \theta) = 0$ for all θ. Hence, it follows that at any level θ_0 at which $u_0^\infty(\theta)$ is positive, then $v_1(\xi, \theta_0) = \Pi_{1\xi} < 0$ for some range(s) of ξ. This means that an efflux of fluid of a given density at the seaward edge of the jet is invariably accompanied by a countercurrent of the same density fluid within the jet. This, of course, is physically necessary for the $v_0 = 0$ jet: the fluid being discharged into the geostrophic interior must come from 'downstream'. If the entire asymptotic velocity profile is eastward, then the entire jet will be flowing southward.

If, instead, the bottom slope is just negative enough so that positive u_0^∞ appears near the bottom only and the transport u_0^∞ remains negative, it is possible to see, in a general way, the region of ξ in which the countercurrent will form. The function Π_1^∞ will be positive over most of its range, going through zero and changing sign near the bottom. For large ξ, the total Π_1-field may be approximated by

$$\Pi_1 \sim A_1 e^{-\lambda_2 \xi} \phi_1(\theta) + \Pi_1^\infty(\theta). \tag{2.93}$$

Since ϕ_1 is the lowest eigenfunction of a S–L system, it will be of one sign in the relevant range of θ, and might as well be taken positive. The coefficient A_1 is given by

$$A_1 = -\left[\int_0^1 \phi_1 \Pi_1^\infty P_0^{-1} d\theta\right] \Big/ \left[\int_0^1 \phi_1^2 P_0^{-1} d\theta\right], \tag{2.94}$$

and it is reasonable to state that for Π_1^∞ mainly positive, A_1 will tend to be negative. If it is assumed $A_1 < 0$, then from (2.93) it follows that as ξ is made smaller, Π_1 will become less positive for all θ until ξ is small enough for the higher eigenfunctions to contribute appreciably to the solution. Thus, in this range of ξ, negative values of u_0 are less negative and positive values more positive than at $\xi = \infty$. Also, $v_1 = \Pi_{1\xi}$ is positive at all levels. Hence the required deep countercurrent will not appear until small values of ξ are reached. It is also seen that there will surely be a countercurrent for some range of θ just above and including the value for which u_0^∞ vanishes, as long as the amount of fluid transported downstream for large ξ exceeds the geostrophic influx. The foregoing analysis, although not rigorous, should alert one to be on the lookout for deep inshore countercurrents in regions where the bottom deepens rapidly enough to admit of deep eastward geostrophic drift at the offshore edge of the stream.

3. Examples of possible boundary currents

It is now appropriate to examine the solutions derived above in greater detail in order to learn to what (if any) extent they are capable of reproducing qualitative features of observed coastal boundary currents.

3.1. *Range of validity of the first-order solutions*

First, it should be clear that the distance downstream for which the first-order solution can be considered a good approximation is strictly limited. For one thing, the driving mass flux from the geostrophic interior may have a significant downstream variation. Similarly, the depth may not be well represented as a linear function of η. Either or both of these effects, which are parameterized by the values of L_0, L_1 and R_2, will enhance the amplitude of the Π_2 field, thus modifying the solution with increasing η. In addition, the basic driving mechanisms themselves, even without the above-mentioned higher-order corrections, will call up second- and higher-order solutions as we proceed downstream, since the amplitude of Π_2 is also a function of K_0, K_1 and R_1. For example, note that inasmuch as u_0 is calculated geostrophically for the $v_0 = 0$ jet, its vanishing at $\xi = 0$ forces the vanishing of ζ_1 (and w_1) there as well. Now, in the model under discussion, the line of intersection of the $\xi = 0$ plane with the bottom must be an isotherm. Thus, for $R_1 \neq 0$, the first-order solution clearly becomes a poor approximation with increasing η. Even for $R_1 = 0$, the first-order solution will be dominant only for $\eta < 1/\beta^*$. Hence, when inquiring into the downstream development of the temperature and velocity fields for various input parameters, one must bear in mind that the range of validity of the first-order solutions, several of which will be displayed graphically below, cannot be determined until further assumptions about the driving mechanisms are made and the resultant second-order problem is solved, although crude upper bounds can be obtained.

3.2. *Limitations of the models studied thus far; the need for numerical solutions*

It is also true that potential vorticity forms studied above, which conveniently lead to analytic solutions to the first-order problem, are not sufficiently general to guarantee a good approximation to oceanic fields. To see this, note that while the basic density stratification is determined by P_0, the asymptotic form of (1.38),

$$P_0 \Pi^{\infty}_{1\theta\theta} - \frac{P_I}{P_0^2} \Pi^{\infty}_1 = -\beta^*, \tag{3.1}$$

or, equivalently,

$$\zeta^{\infty}_{1\theta} = u^{\infty}_{0\theta\theta} = \frac{1}{P_0}\left[\frac{P_I}{P_0^2} u^{\infty}_0 + \beta^*\right], \tag{3.2}$$

clearly shows that the downstream variation of the stratification ζ^{∞}_1 is a function of P_I as well as P_0. Hence, while it is possible to model a realistic thermocline structure well at a given latitude by taking $P = P_0 = \theta^2/p\,(p+1)$ and judiciously choosing p, it is generally impossible to get more than one isotherm slope correctly with a given choice of K_0 and K_1. This is so because with the particular choice $P_I = 0$, both ζ^{∞}_0 and $\zeta^{\infty}_{1\theta}$ are determined solely by P_0 and therefore cannot be chosen independently. On the other hand, even as simple a form as $P = 1 + C\psi\,(C = \pm\alpha^2)$ permits a rather good representation of isotherm slopes over the entire depth interval for the right value of C. However, the resultant linear basic stratification is not realistic. Thus, it is necessary to have both $P_0 = P_0(\theta)$ and a non-zero P_I (preferably also a function of θ) to model properly the asymptotic density and velocity fields.

Despite this shortcoming, the forms of P we have considered *are* capable of describing a wide range of qualitatively different asymptotic fields. In the simplest such case, i.e. constant potential vorticity in a flat-bottomed ocean, there must be a spreading of the isotherms downstream and a positive value for $u^{\infty}_{0\theta\theta}$ or $u^{\infty}_{0\zeta\zeta}$. The same restrictions on $\zeta^{\infty}_{1\theta}$ and $u^{\infty}_{0\theta\theta}$ will hold for any $P = P_0(\theta) > 0$, but the corresponding $\zeta_0(\theta)$ relationship may permit $u^{\infty}_{0\zeta\zeta}(\theta)$ to take on negative values. Examples of this are displayed in figures 7 and 16 below. The downstream spread of isotherms is required for any $P_I \leqslant 0$ as (3.2) clearly shows (recall $u^{\infty}_0 < 0$ for flat bottom). However, choosing $P_I > 0$ suggests the possibility of relaxing this constraint. In fact, the choice $K_0 < 0 < K_1$ (in the region that becomes permitted for $P = 1 + \alpha^2\psi$), coupled with the $\Pi^{\infty}_1 > 0$ constraint, insures a downstream convergence of isotherms and a region of negative $u^{\infty}_{0\zeta\zeta}$. Hence, various combinations of density and velocity fields can be approximated using the four simple forms for P, and it should therefore be possible to obtain first-order solutions that exhibit qualitative features of oceanic coastal jets.

To obtain better than a qualitative agreement, P_0 and P_I must be chosen as realistically as possible. This will almost surely involve θ-dependences that not only do not lead to analytic solutions but that likely are not expressible in terms of simple functions. However, numerical solutions should be obtainable without undue difficulty. In fact, the use of numerical techniques in conjunction with high-speed computers is clearly required to obtain realistic coastal jet solutions. This is because: (*a*) neither the Florida Current nor the Kurishio Current satisfy well the $v_0 = 0$ hypothesis, they already exist as free jets before they begin flowing along a western boundary (possibly the best example of a $v_0 = 0$ coastal jet is the East Australia Current, but there is a scarcity of temperature–salinity data near the region of formation, 15°–25° S. lat.), and (*b*) the bottom topography is generally not independent of the cross-stream co-ordinate, a fact that leads to a modification of the jet structure, especially adjacent to the coast (see Niiler & Spiegel 1968). Both of these features preclude the possibility of a $\theta - \xi$ separation of variable and confound attempts to find analytic solutions. Hence, a logical next step is a numerical solution of the $v_0 \neq 0$ equations with realistic driving fluxes and boundary conditions. For the present, however, an inspection of several examples of the types of geostrophic drift consistent with forming a $v_0 = 0$ coastal jet and a detailed examination of the resultant jet structure for some of these, must suffice.

3.3. *Discussion of several solutions*

The solutions to be exhibited were obtained with the aid of the Harvard Computing Centre's IBM 7094 Data Processing System. Eigenvalues were computed to at least four significant figures, and the machine was programmed to calculate the expansion coefficients and sum the requisite series to produce the fields of interest. Enough terms were taken so that the boundary conditions were satisfied to tenths of a per cent, and the last term included did not affect the first two figures of the answers (these criteria were relaxed somewhat in the neighbourhood of $\xi = 0$, $\theta = b_0$ for $R_1 \neq 0$).

Figures 7 and 8 show (in non-dimensional units) the asymptotic fields only of

several possible first-order solutions, illustrating to some extent the wide variety of jets capable of description by our model. Figures 9–17 show the full velocity and density fields associated with nine different first-order solutions. They were selected because they exhibit qualitatively some of the observed features of the

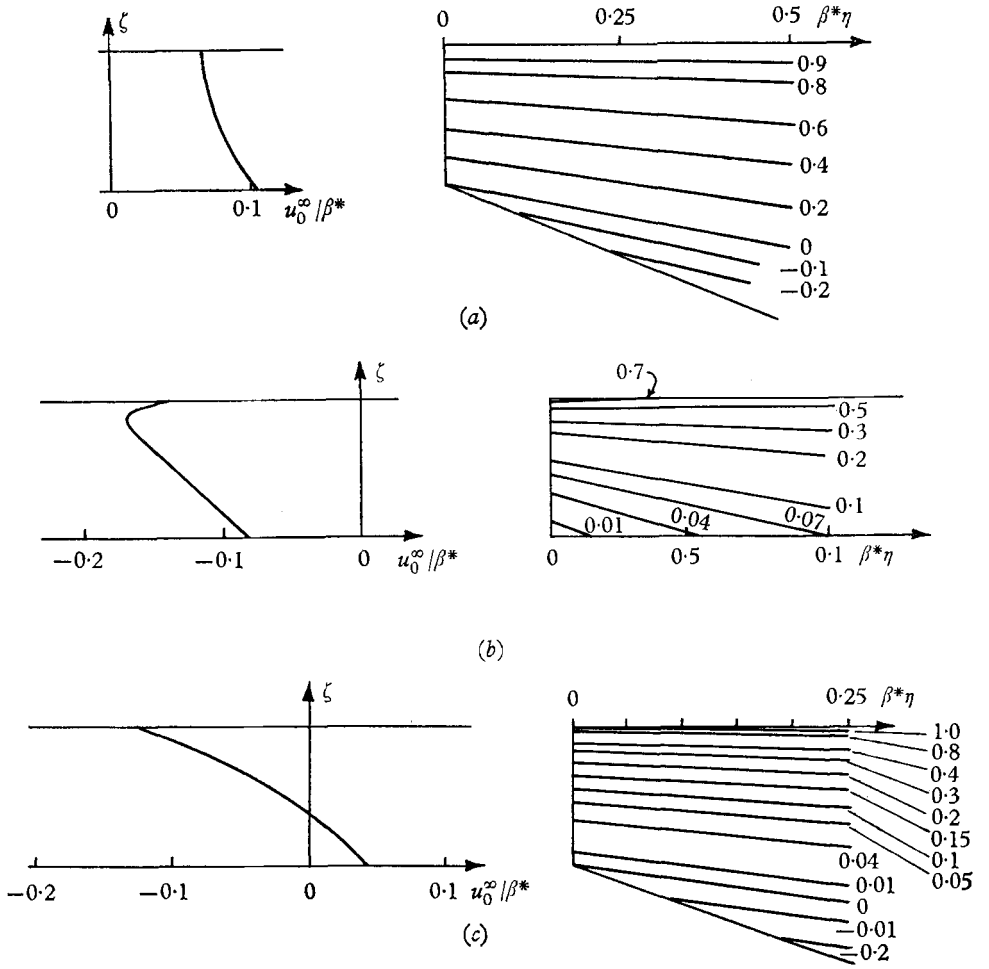

FIGURE 7. Asymptotic velocity and density profiles for the cases:
(*a*) $P = 1$, $K_0 = 1$, $K_1 = 10$, $R_1 = -2\beta^*$, $U_0^\infty = 0{\cdot}760\beta^*$;
(*b*) $P = \theta^2/0{\cdot}11$, $K_0 = 0{\cdot}1$, $K_1 = -1$, $R_1 = 0$, $U_0^\infty = -0{\cdot}134$;
(*c*) $P = \theta^2/0{\cdot}11$, $K_0 = 0{\cdot}02$, $K_1 = 10$, $R_1 = -3\beta^*$, $U_0^\infty = -0{\cdot}0298\beta^*$.

Florida Current as it flows over the Blake Plateau: gradual spreading and deepening of the isotherms downstream, and greatest horizontal velocities near the surface.

(*a*) *Flat-bottom currents with linear basic stratification*

The first three examples, shown in figures 9–11, are solutions for purely baroclinic jets, i.e. jets with $u_0^\infty(0) = v_1^\infty(0) = K_0 = 0$ for the cases $P = 1$, $1+\psi$ and $1-\psi$, respectively. The K_1 values have been chosen to make $u_0^\infty(1) = 1$. The

curvature in u_0^∞, and thus the spread of isotherms, is greatest for $P = 1-\psi$ and least for $P = 1+\psi$, whereas the downstream rise in surface temperature is greatest for the latter and least (almost non-existent) for the former. The v_1 and w_1 contours are all quite similar, the degree of curvature of profile varying

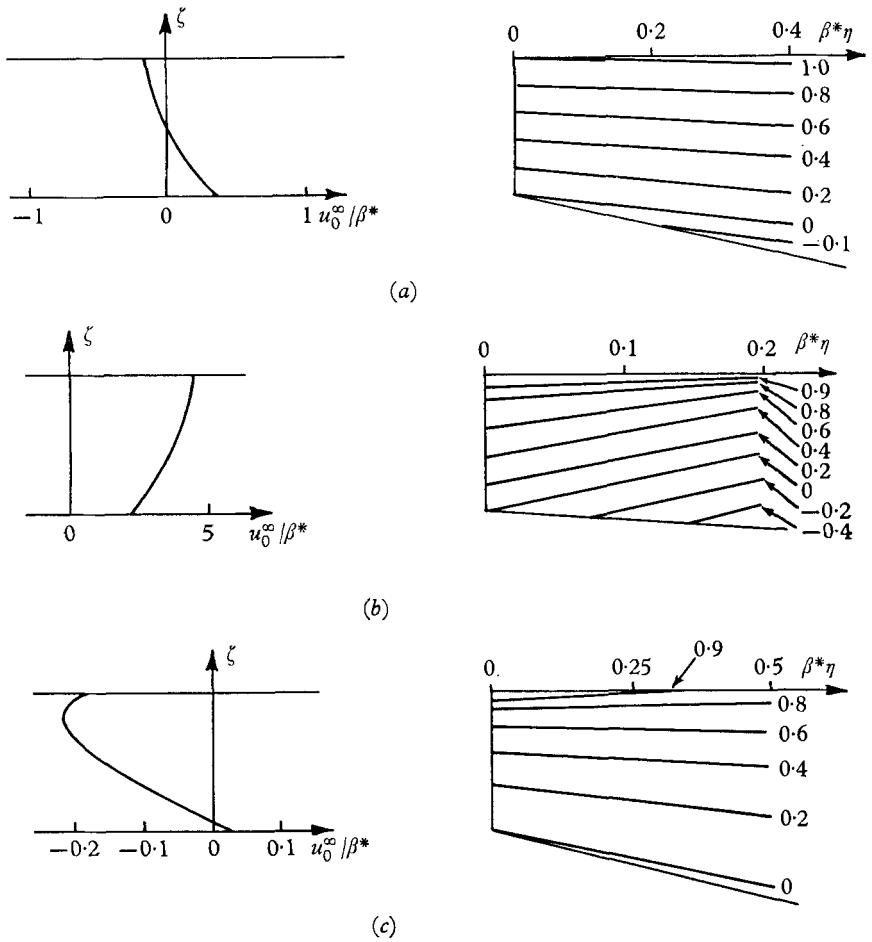

FIGURE 8. Asymptotic velocity and density profiles for the cases:
(*a*) $P = 1+\psi$, $K_0 = 0{\cdot}4$, $K_1 = 1{\cdot}6$, $R_1 = -2\beta^*$, $U_0^\infty = -0{\cdot}0243\beta^*$;
(*b*) $P = 1-\psi$, $K_0 = 0{\cdot}6$, $K_1 = 10$, $R_1 = -\beta^*$, $U_0^\infty = 3{\cdot}733\beta^*$;
(*c*) $P = \theta^2/2$, $K_0 = 0{\cdot}1$, $K_1 = -1$, $R_1 = -\beta^*$, $U_0^\infty = -0{\cdot}139\beta^*$.

with that of u_0^∞. The v_1 field is always positive for $\zeta > 0$, having its maximum at the surface adjacent to the coast; while w_1, which is also always positive (except that it vanishes at $\xi = \zeta = 0$ and $\zeta = 1$), takes on its maximum value at approximately $\xi = \zeta = 0{\cdot}6$. Of course, this upwelling everywhere results solely from the types of asymptotic fields considered and is not at all a necessary feature of coastal jets. This immediately follows from the fact that for all jets with $P_0 = 1$ and $R_1 = 0$, an interchange of the values K_0 and $-K_1$ results in a reflexion of the fields about the plane $\theta = 0{\cdot}5$, thus giving jets with $w_1 < 0$ for the examples just

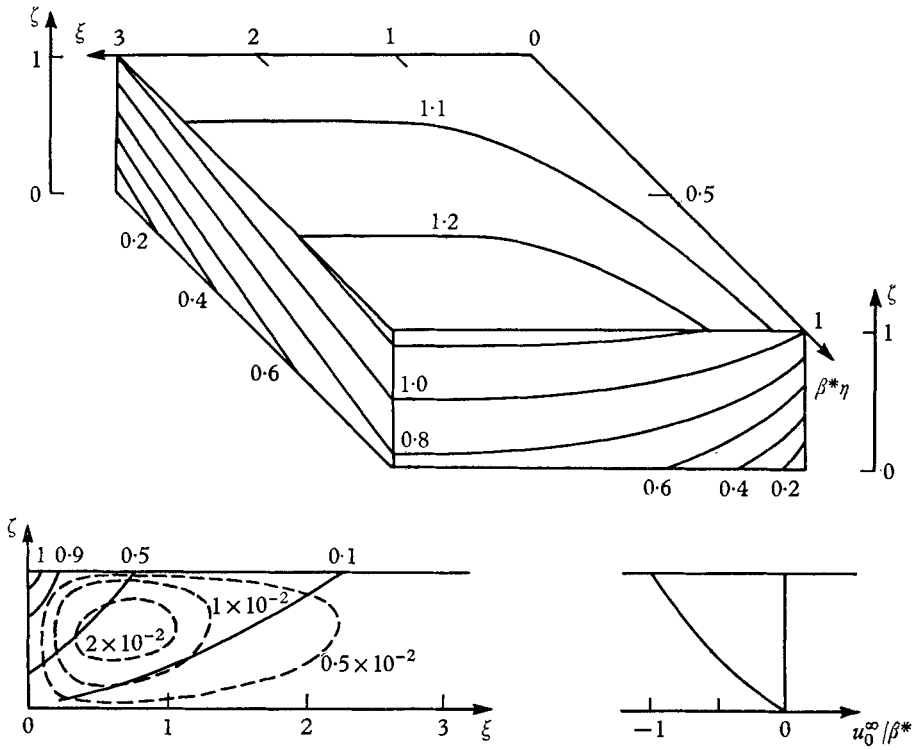

FIGURE 9. Velocity and density fields for a baroclinic jet with $P = 1$, $K_0 = 0$, $K_1 = 2$, $U_0^\infty = -0{\cdot}583\beta^*$. ——, v_1/β^*; – – –, w_1/β^{*2}.

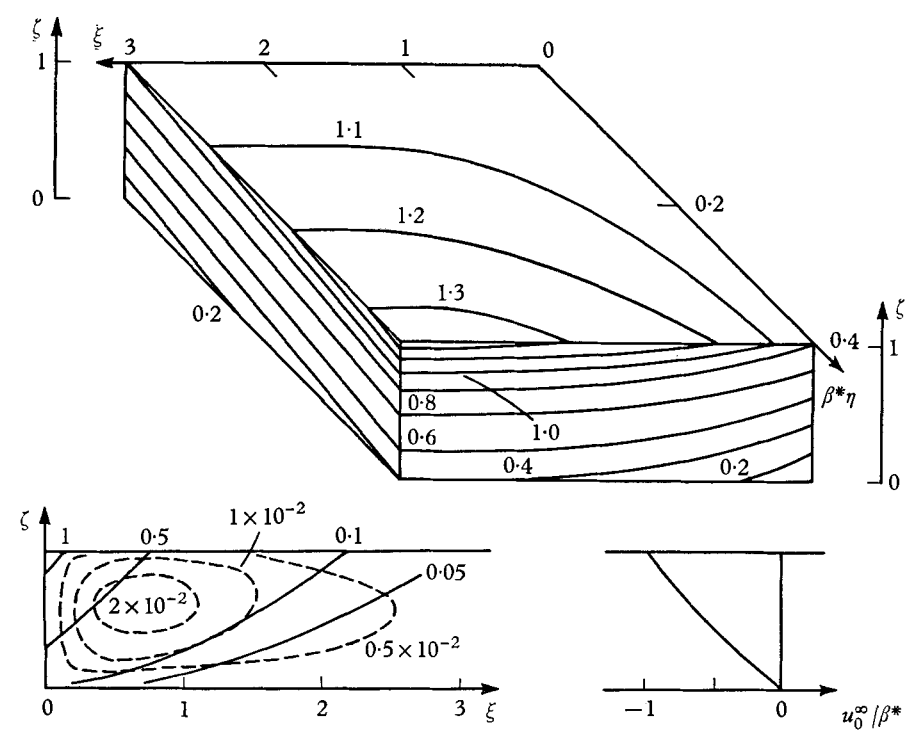

FIGURE 10. Velocity and density fields for a baroclinic jet with $P = 1+\psi$, $K_0 = 0$, $K_1 = 1{\cdot}176$, $U_0^\infty = -0{\cdot}537\beta^*$. ——, v_1/β^*; – – –, w_1/β^{*2}.

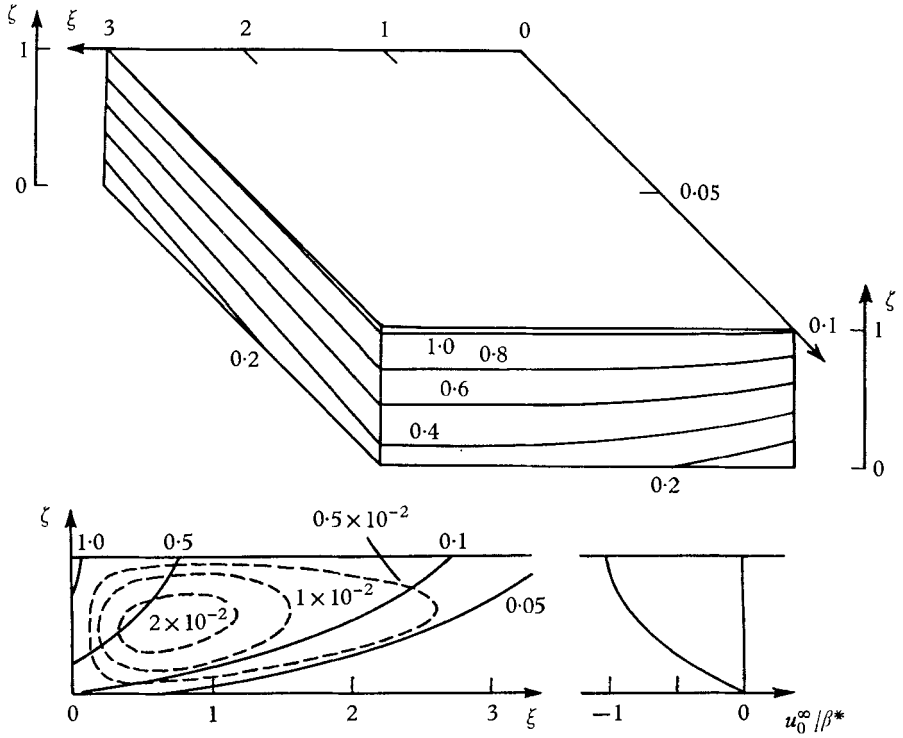

FIGURE 11. Velocity and density fields for a baroclinic jet with $P = 1-\psi$, $K_0 = 0$, $K_1 = 10$, $U_0^\infty = -0{\cdot}643\beta^*$. ——, v_1/β^*; – – –, w_1/β^{*2}.

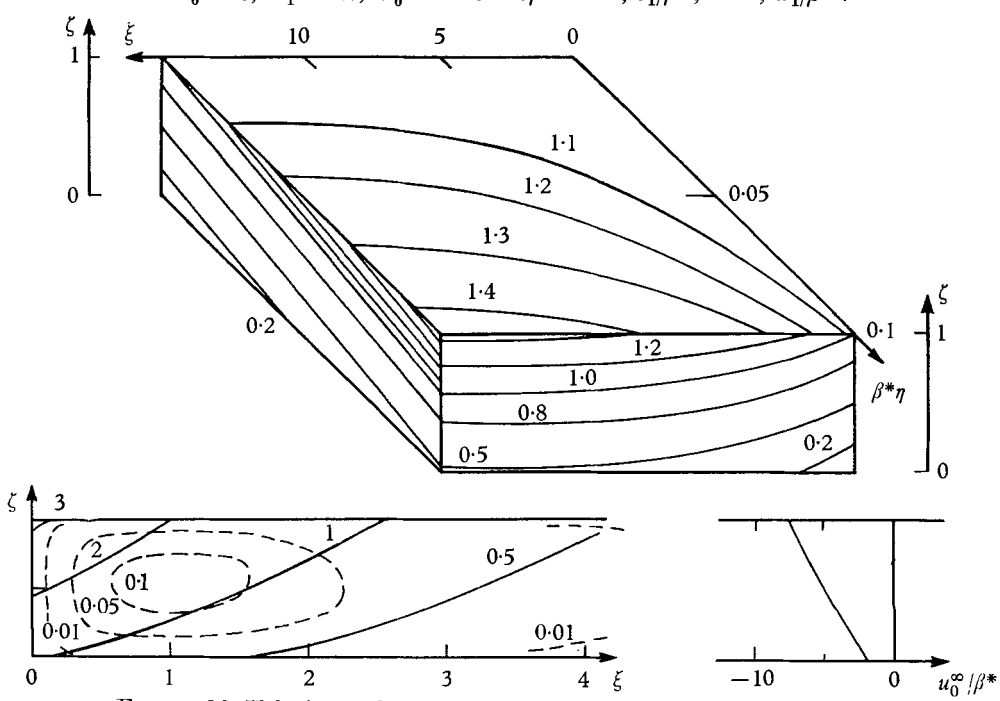

FIGURE 12. Velocity and density fields for $P = 1$, $K_0 = 0{\cdot}4$, $K_1 = 1{\cdot}6$, $R_1 = 0$, $U_0^\infty = -4{\cdot}783\beta^*$. ——, v_1/β^*; – – –, w_1/β^{*2}.

considered. Also, note that the small amplitude of w_1 (relative to that of u_0 and v_1) in these and succeeding examples results from the consideration of only cases with gently sloping asymptotic isotherms, especially at levels where u_0^∞ is large.

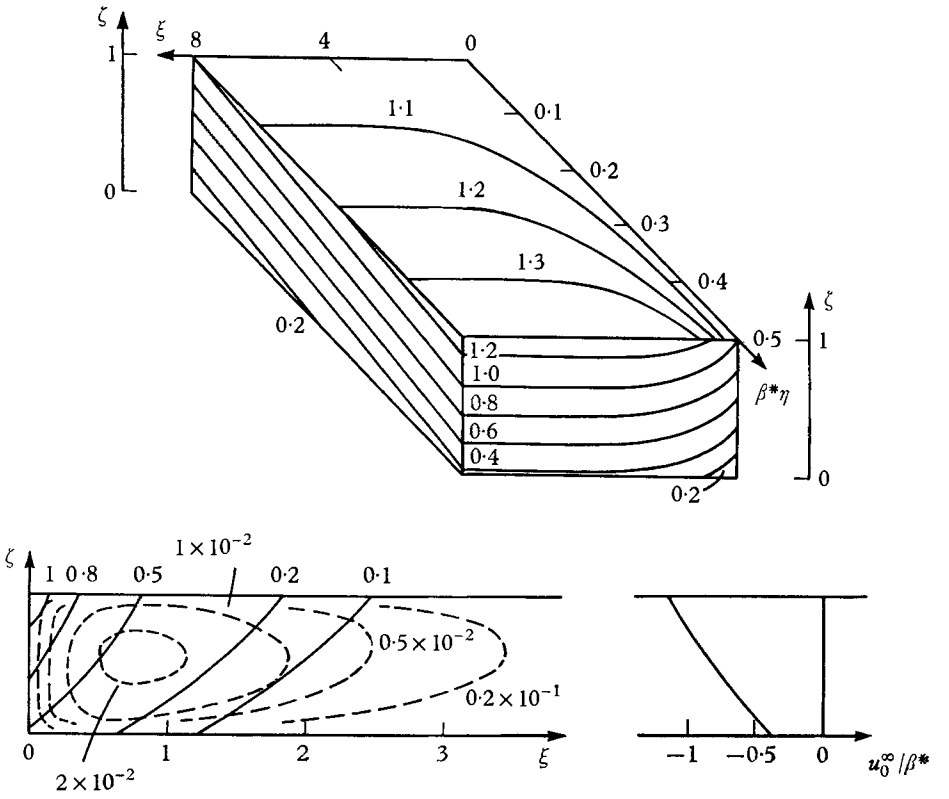

FIGURE 13. Velocity and density fields for $P = 1+\psi$, $K_0 = 0{\cdot}4$, $K_1 = 1{\cdot}6$, $R_1 = 0$, $U_0^\infty = -0{\cdot}773\beta^*$. ——, v_1/β^*; – – –, w_1/β^{*2}.

The next two solutions (figures 12 and 13) are for constant depth jets with $u_0^\infty(0)$ non-zero and increasing monotonically with height (or density) for constant potential vorticity and for $P = 1+\psi$. Except for the fact that $v_1(0) \neq 0$, the v_1 and w_1 fields do not differ qualitatively from those considered above. However, for the example of figure 18, the asymptotic isotherms, which always deepen downstream, converge for $\theta > 0{\cdot}8$ and diverge for $\theta < 0{\cdot}8$, thus indicating a rather modest thermocline development downstream.

(*b*) *Current with* $u_0^\infty(0) > 0$

The next to be considered is a CPV model with the parameters so chosen that the u_0^∞ profile has a positive region near the ocean bottom. In order to see whether the selected bottom slope, $R_1 = -2\beta^*$, is consistent with topography of the real ocean basin, the values of the scaling parameters must be specified. Typical values in the vicinity of the Blake Plateau are: $U_0 = 10$ cm sec^{-1}, $H = 5 \times 10^4$ cm,

$\Delta\rho/\rho = 4\times10^{-3}$, $g = 10^{-3}$ cm sec^{-2}, $f_0 = 6\times10^{-5}$ sec^{-1}, $\beta = 2\times10^{-13}$ cm^{-1} sec^{-1}, and $\Theta \approx 0$. These lead (see IC) to a downstream scale length of 300 km, a cross-stream scale length of 60 km, scales for v and w of 450 cm sec^{-1} and 0·08 cm sec^{-1}, respectively, and a value for β^* of 0·8. The cross-stream length is a reasonable Gulf Stream value, while the fact that the upwelling scale is some 3 to 4 orders of magnitude greater than that of the oceanic Ekman divergence lends credence to the neglect of surface wind stress in the model. Even the large downstream velocity scale leads to no unreasonable high velocities (as long as $v_1 \lesssim 1$), since the distance from the Florida Straits to Cape Hatteras corresponds to a range in η of only $\frac{1}{3}$. The physical value of the bottom slope $\Delta z/\Delta y$ is readily calculated from the relation,

$$\frac{\Delta z}{\Delta y} = \frac{H}{L}R_1 = \frac{R_1\beta}{\beta^* f_0}H; \tag{3.3}$$

for the given values, a slope of $R_1 = -2\beta^*$ yields a physical slope of -3×10^{-4}. Since slopes of the order of tenths of a per cent are common parallel to the coast on the Blake Plateau, the value associated with the jet being discussed is by no means unrealistic.

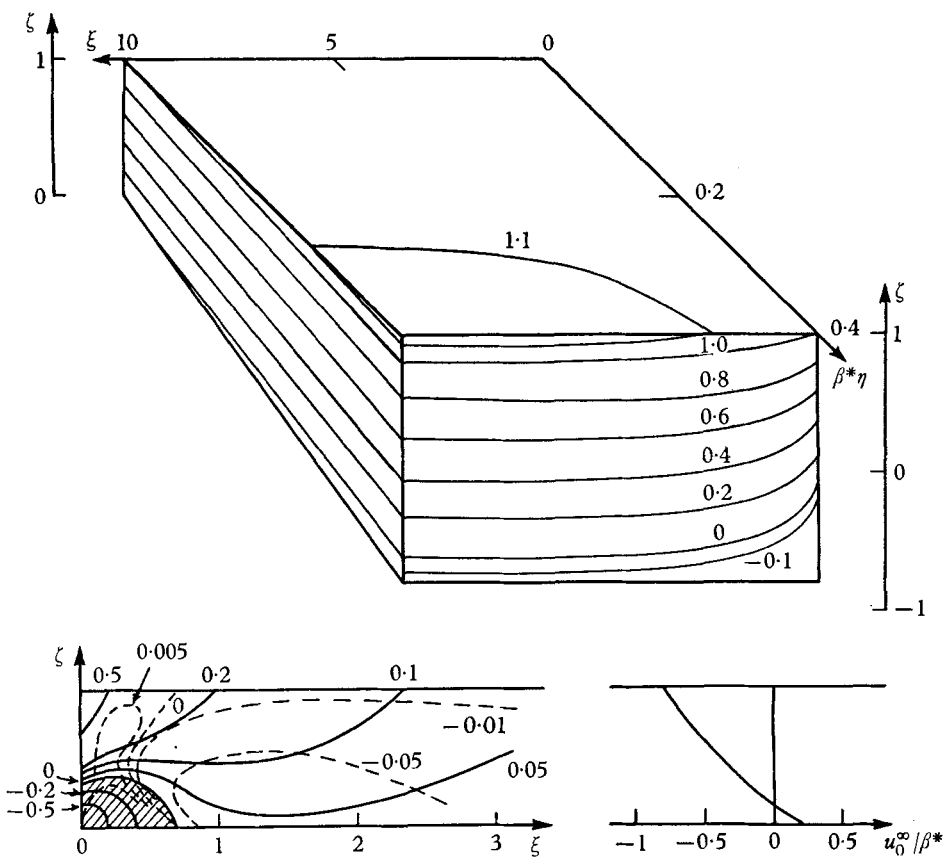

FIGURE 14. Velocity and density fields for $P = 1$, $K_0 = 0{\cdot}4$, $K_1 = 1{\cdot}6$, $R_1 = -2\beta^*$, $U_0^\infty = -0{\cdot}383\beta^*$. The v_1 countercurrent region is shaded.

The v_1 field is seen (figure 14) to have the necessary deep countercurrent; indeed, it is tucked against the coast as we anticipated. Not surprisingly negative v_1 values persist for values of θ greater than those for which u_0^∞ is positive. This suggests the possibility of choosing parameters such that a countercurrent exists, even if $u_0^\infty < 0$ at all levels. (In fact, such a case is exhibited in figure 15 below.) In all the previous solutions, for a given θ, v_1 took on its maximum (positive) value at $\xi = 0$; in the present example, this clearly is not so. Also, for the first time, w_1 takes on both signs; by virtue of the kinematic lower boundary condition, this must occur whenever a current–countercurrent system impinges on a sloping bottom.

Once numerical values for the scaling parameters are introduced, they can be inserted in the non-dimensional solutions to obtain physical density and flow fields. A variation of the values of $\Delta\rho/\rho_0$ and H will relate the solutions to other inlet conditions. It should be noted that for a given physical slope (i.e. $R_1/\beta^* =$ const.), changing the value of U_0 only does not alter the physical fields at all; the scalings of u, v, w and ζ, coupled with the values of β^* and L, are such that the parameter U_0 cancels out of the problem, with the natural scale for the cross-stream velocity component being given by $(\Delta\rho/\rho_0)gH\beta^*/f_0^2$. This result, which is traceable to the absence of u in the conservation of potential vorticity equation,

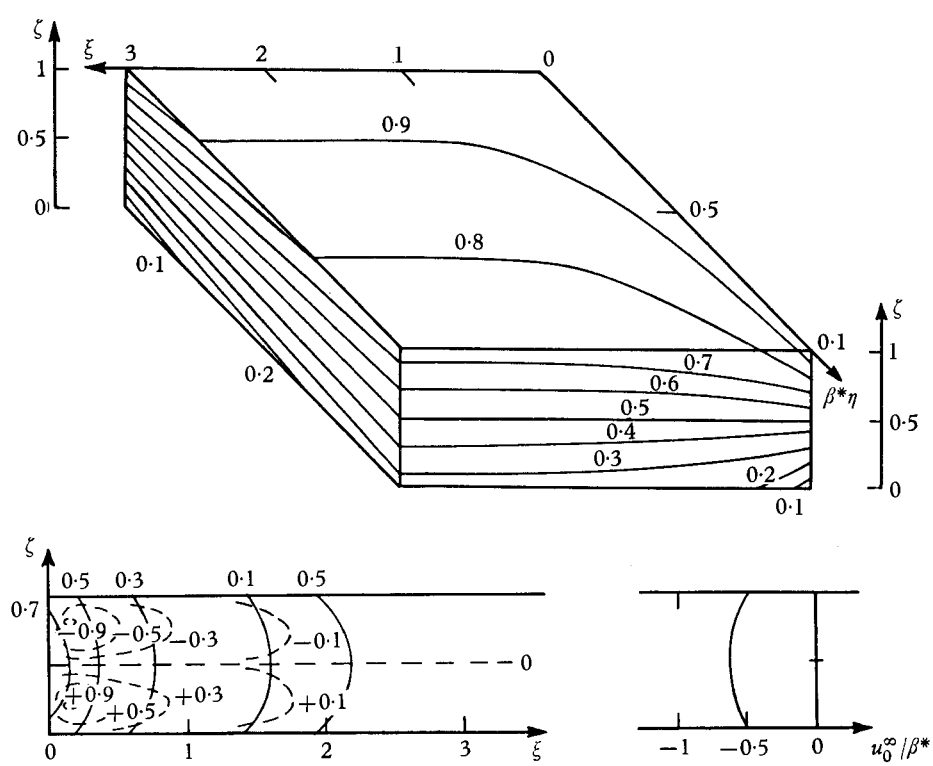

FIGURE 15. Velocity and density fields for an asymptotic profile symmetric about $\zeta = 0{\cdot}5$, with $P = 1$, $K_0 = 1$, $K_1 = -1$, $R_1 = 0$ and $U_0^\infty = -0{\cdot}583\beta^*$. The symmetry permits a splitting of the solution into upper and lower non-communicating halves ($K_{0.5} = -\infty$). ——, v_1/β^*; – – –, $10^2 \times w_1/\beta^{*2}$.

means that for given $\Delta\rho/\rho_0$, H and R_1/β^*, the physical value of the driving mass flux can be varied only by the choice of new values of K_0 and K_1; thus a new first-order solution would be needed to find the resultant jet structure.

(*c*) *Current with symmetric u_0^∞; second-order solution*

The next example (figure 15) has a symmetric u_0^∞ and is thus, in a sense, the closest approximation to a barotropic driving mass flux permitted at CPV in a stratified flow. Since $R_1 = 0$, the fields are completely symmetric about the constant temperature surface $\zeta = 0{\cdot}5$; thus, the upper-half solution and its mirror-image lower half are themselves valid solutions to the problem where one of the horizontal bounding surfaces is isothermal ($K_{0{\cdot}5} = -\infty$). In order to get some quantitative idea as to the distance downstream at which the first-order solution is no longer dominant, the second-order solution for this example has been calculated for the case of vanishing first-order geostrophic transport u_1^∞ (corresponding to a minimal perturbation of the system). The parameters are $K_0 = 1$, $K_1 = -1$, $L_0 = L_1 = -\frac{19}{3}$, $R_1 = R_0 = 0$. The solution is found to be:

$$\begin{aligned}
\Pi_1 &= \beta^*\{0{\cdot}5[1+\theta-\theta^2] - [0{\cdot}4979\, e^{-1{\cdot}307\xi}\phi_1(\theta) \\
&\quad + 0{\cdot}0019\, e^{-6{\cdot}584\xi}\phi_3(\theta) + 0{\cdot}0007\, e^{-12{\cdot}723\xi}\phi_5(\theta) + \ldots]\}, \\
\Pi_2 &= \beta^{*2}\{0{\cdot}5833 - 1{\cdot}3125\, e^{-1{\cdot}307\xi} + 0{\cdot}3021\, e^{-2{\cdot}614\xi} \\
&\quad + [(0{\cdot}2007 - 0{\cdot}0782\xi)\, e^{-1{\cdot}307\xi} - 0{\cdot}3423\, e^{-2{\cdot}614\xi}]\phi_1(\theta) \\
&\quad + [0{\cdot}0859\, e^{-6{\cdot}584\xi} - 0{\cdot}00462\, e^{-1{\cdot}307\xi} + 0{\cdot}00485\, e^{-2{\cdot}614\xi}]\phi_3(\theta) \\
&\quad + [0{\cdot}0215\, e^{-12{\cdot}723\xi} - 0{\cdot}000354\, e^{-1{\cdot}307\xi} + 0{\cdot}000337\, e^{-2{\cdot}614\xi}]\phi_5(\theta) + \ldots\},
\end{aligned}$$

where

$$\phi_n = \cos\lambda_n\theta + \lambda_n^{-1}\sin\lambda_n\theta, \quad \lambda_1 = 1{\cdot}307, \quad \lambda_3 = 6{\cdot}584, \quad \lambda_5 = 12{\cdot}723.$$

The v_1 and v_2 fields are calculated according to (1.29) and (1.30) and are found to yield physical velocities that are equal in magnitude for $\eta \sim 0{\cdot}8/\beta^*$. This is so, even though the ratio of the amplitudes of the driving mass fluxes $|u_1^\infty\eta|/|u_0^\infty|$ is, at most, equal to $\frac{1}{6}\beta^*\eta$. Hence, it is seen that second-order corrections will indeed become important even in a region where modifications of the driving terms are very small. A second example has been solved for the case $L_0 = L_1 = 0$ for which $u_1^\infty > 0$ everywhere; here, both $|v_2|/|v_1|$ and $|u_{1\theta}^\infty|/|u_0^\infty|$ indicate convergence for $\eta < \frac{1}{3}/\beta^*$.

(*d*) *Current with thermocline structure*

The next first-order solution is the case $P = \theta^2/1{\cdot}1$, i.e. $p = 0{\cdot}1$. This leads to the thermoclinic zero-order stratification $\theta = 0{\cdot}11/(1{\cdot}1-\zeta)$. In figure 16, the lines of constant density are labelled with the values $\theta - p$ so that the density range at $\eta = 0$ will run from 0 to 1. Note that u_0^∞ has considerable *negative* curvature in physical space, while $v_1|_{\xi=0}$ increases almost linearly with ζ. In density space, $u_{0\theta\theta}^\infty$ is positive (as it must be) and the $v_1|_{\xi=0}$ profile is similar in shape, although opposite in sign, to that of u_0^∞. The asymptotic density field, with its gently deepening thermocline structure, is qualitatively reminiscent of meridional temperature sections in the interior North Atlantic in the latitude

range of the Blake Plateau (Fuglister 1960, pp. 49 and 51) and consistent with observations in the Florida Current (Iselin 1936, pp. 60–9). Unfortunately, a choice of parameters p, K_0, K_1 and R_1 that well represents the observed density and bottom topography gives a u_0^∞ scale leading to transports that are an order of magnitude too small, whereas a choice of K_0 and K_1 that yields a realistic transport is descriptive of excessively downward sloping density surfaces at the jet's seaward edge. The arbitrary choice $P_I = 0$ is simply not descriptive of the Florida Current.

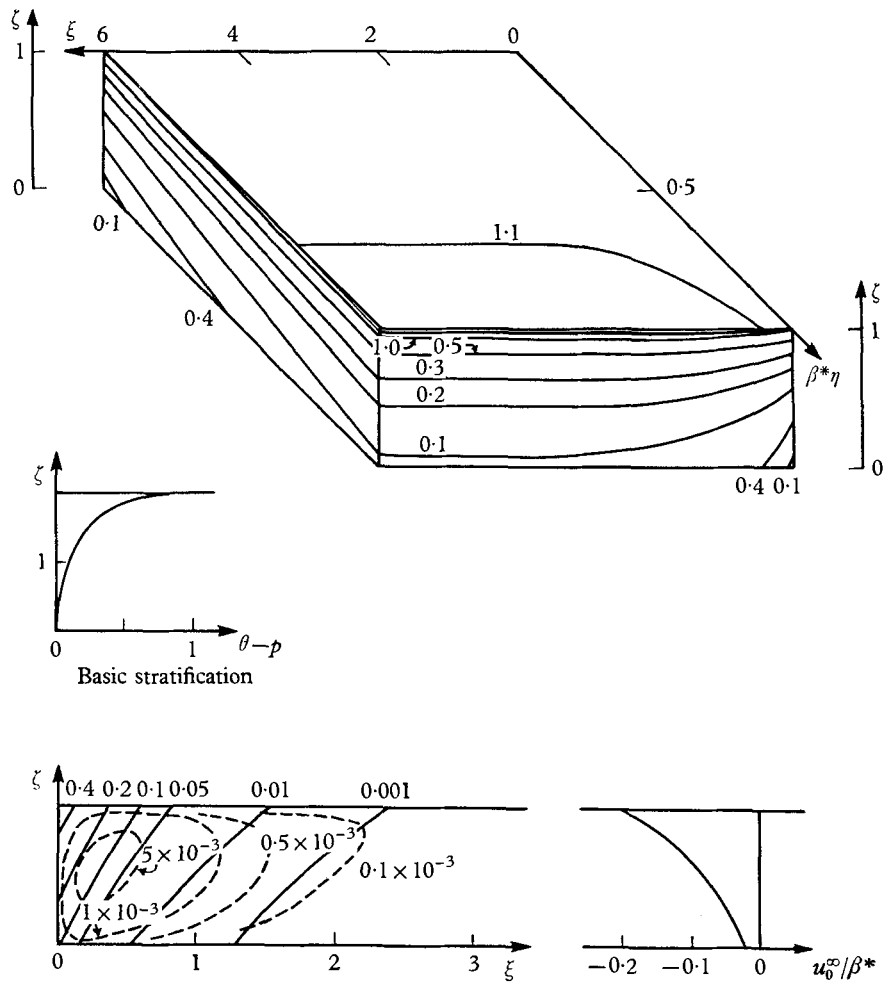

FIGURE 16. Velocity and density fields for $P = \theta^2/0{\cdot}11$, $K_0 = 0{\cdot}02$, $K_1 = 10$, $R_1 = 0$, $U_0^\infty = -0{\cdot}091\beta^*$. ——, v_1/β^*; – – –, w_1/β^{*2}.

3.4. *Model for the Florida current; concluding remarks*

Accordingly, a compromise is made by accepting a linear basic stratification and seeking the best 'fit' from the remaining forms of the potential vorticity functional. The choice $P = 1-\psi$, $K_0 = 0{\cdot}1$, $K_1 = 3{\cdot}0$, $R_1 = -2\beta^*$ leads to a solution that is about as realistic as can be obtained with the available forms for P. The

various fields are displayed in non-dimensional units in figure 17, which is labelled for the specific choice $\beta^* = 0{\cdot}8$. The parameters were selected to try to match the solution's transport and cross-stream density sections at $\eta = 0{\cdot}25$ and $0{\cdot}375$ with those of the Florida Current off Cape Kennedy (formerly Cape Canaveral) and Jacksonville, respectively. The latter sections were calculated from temperature and salinity sections given by Iselin (1936) in his figures 41 and 43. With Iselin's figure 48 serving as a rough guide, the model has been

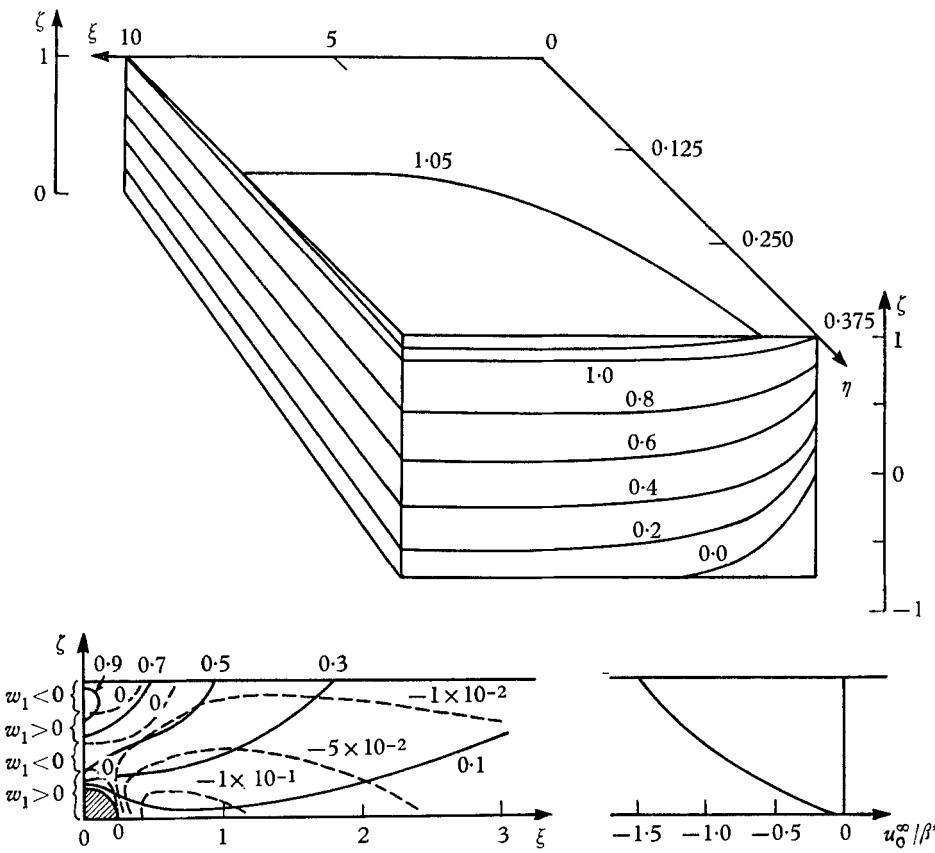

FIGURE 17. Velocity and density fields for $P = 1-\psi$, $K_0 = 0{\cdot}1$, $K_1 = 3{\cdot}0$, $R_1 = -2\beta^*$, $\beta^* = 0{\cdot}8$, $U_0^\infty = -0{\cdot}899$. The v_1 countercurrent region is shaded. ——, v_1; – – –, w_1.

adjusted to give a transport of 27×10^6 m^3 sec^{-1} at Cape Kennedy and 40×10^6 m^3 sec^{-1} at Jacksonville. A comparison of the theoretical and observed density sections is given in figures 18 and 19. Apart from the inherent lack of thermocline structure, the model is seen to survive the comparison fairly well. The (negative) slopes of the isopycnals as they leave the coast steepen with depth in both model and ocean, and even the slight levelling off of the slopes of the deeper oceanic isopycnals at the coast is mirrored to an extent in the solution. It is this levelling off that is associated with the deep onshore countercurrent shown in figure 17. Whether this countercurrent would still appear in the solution if more realistic values of cross-stream topography and stratification were incorporated

in the model is not clear. The authors are unaware of any measurements either affirming or denying the existence of such a countercurrent at the points in question.

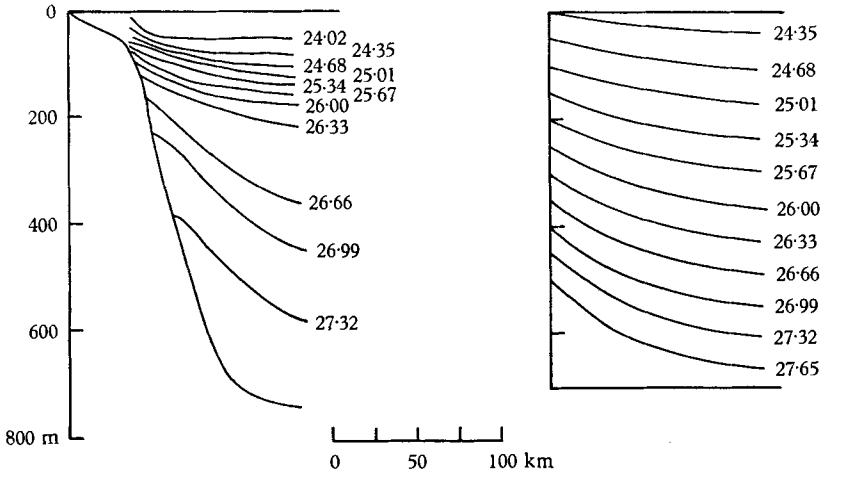

FIGURE 18. Sigma-T values for a cross-section of the Florida Current off Cape Kennedy (formerly Cape Canaveral) plotted at left, compared with values given by the model of figure 20 at $\eta = 0{\cdot}25$.

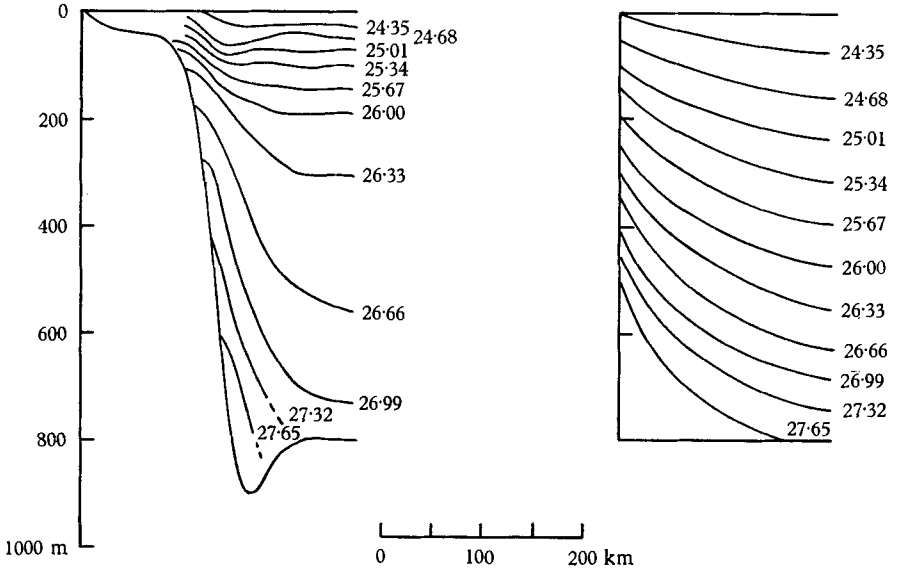

FIGURE 19. Sigma-T values for a cross-section of the Florida Current off Jacksonville plotted at left, compared with values given by the model of figure 20 at $\eta = 0{\cdot}375$.

However, there is little purpose in making a detailed survey of the points of agreement and discrepancy between our model and the Florida Current. The model is admittedly crude; in order to circumvent the restrictive $v_0 = 0$ approximation, the origin of the downstream expansion has been taken half-way between

the southern tip of Florida and Cuba. Also, it is clear that the second-order terms in the expansion must be of importance at $\eta = 0{\cdot}3$ since, there, the depth has increased by a factor of 8/5 from its initial value. What should really be done is to place the origin of the expansion at the $v_0 \neq 0$ Cape Kennedy section and, with more realistic values of $P(\theta, \psi)$ and $R_1(\xi)$, see how closely the inertial model forecasts the physical situation at Jacksonville. Such a numerical investigation is now in progress.

Appendix. By S. L. Spiegel

For the various simple potential vorticity distributions studied in this paper and in IC, it has always been found that in a constant depth ocean, the formation of an inertial boundary current required a seaward geostrophic drift that was westward at all levels. That this restriction might hold generally for inertial coastal jets was strongly suggested by a calculation presented in the closing section of IC. It is the purpose here to prove that this constraint holds for arbitrary potential vorticity for the $v_0 = 0$ jet.

The relevant differential equation is

$$\Pi_{1\xi\xi} + P_0 \Pi_{1\theta\theta} - \frac{P_I}{P_0^2} \Pi_1 = -\beta^*, \tag{A 1}$$

with boundary conditions (1.39)–(1.42). Here, P_I is an arbitrary function of θ, but the requirement of stable stratification implies $P_0(\theta) > 0$, $0 \leqslant \theta \leqslant 1$. Let

$$\Pi_1(\xi, \theta) = \sum_n e^{-\lambda_n \xi} \phi_n(\theta) + \Pi_1^\infty(\theta). \tag{A 2}$$

This leads to the equations

$$\mathscr{L}(\Pi_1^\infty) \equiv \left[-\frac{d^2}{d\theta^2} + \frac{P_I}{P_0^3} \right] \Pi_1 = \frac{\beta^*}{P_0} > 0, \tag{A 3}$$

$$K_0 \Pi_1^{\infty\prime}(0) - \Pi_1^\infty(0) = K_1 \Pi_1^{\infty\prime}(1) - \Pi_1^\infty(1) = 0 \tag{A 4}$$

and

$$\mathscr{L}(\phi_n) = \Lambda_n \phi_n / P_0, \tag{A 5}$$

$$K_0 \phi_n'(0) - \phi_n(0) = K_1 \phi_n'(1) - \phi_n(1) = 0, \tag{A 6}$$

where

$$\Lambda_n \equiv \lambda_n^2. \tag{A 7}$$

The equations for the ϕ_n are of Sturm–Liouville form, with eigenvalues Λ_n, provided $P_0(\theta) > 0$.

Now in order for there to be a boundary current, it is necessary for all the λ_n to be real; thus the Λ_n must all be positive. One way to get an upper bound for the lowest eigenvalue Λ_1 is to select a normalized trial function $F(\theta)$ that satisfies the boundary conditions on the ϕ_n and calculate the Rayleigh integral,

$$I_R \equiv \int_0^1 F \mathscr{L}(F)\, d\theta;$$

it is known from S–L theory that $\Lambda_1 \leqslant I_R$.

Let $G(\theta)$ be the normalized form of Π_1^∞:

$$G = N\Pi_1^\infty(\theta), \tag{A 8}$$

$$N = \left[\int_0^1 (\Pi_1^{\infty 2}/P_0)\,d\theta\right]^{-\frac{1}{2}}. \tag{A 9}$$

Since G satisfies the ϕ_n boundary conditions, it can be used as a trial function to get an upper bound for the lowest eigenvalue Λ_1:

$$\begin{aligned}\Lambda_1 &\leqslant \int_0^1 G\mathscr{L}(G)\,d\theta \\ &= N^2\int_0^1 \Pi_1^\infty \mathscr{L}(\Pi_1^\infty)\,d\theta \\ &= N^2\beta^*\int_0^1 (\Pi_1^\infty/P_0)\,d\theta,\end{aligned} \tag{A 10}$$

where use has been made of (A 3). Thus, no boundary current will form if the right-hand side of (A 10) is negative. The quantities β and N^2 are both positive. Since $\Pi_1^\infty = -u_0^\infty$ and $P_0^{-1} = \zeta_{0\theta}$, the last condition can be restated in the form

$$\int_0^1 u_0^\infty\,d\zeta_0 < 0 \tag{A 11}$$

for the existence of a coastal boundary current. In other words, in the absence of bottom topography, the inertial jet must receive an influx of fluid at its seaward edge.

The question now arises whether or not there can be an efflux of fluid into the ocean's interior at any level and still maintain a boundary current. Equivalently, one may inquire if it is possible to have $\Lambda_1 > 0$ if $\Pi_1^\infty(\theta)$ is negative anywhere in the interval $0 \leqslant \theta \leqslant 1$. The answer is that it is not possible; for any Π_1^∞ that takes on negative values, a trial function F can be constructed such that

$$\int_0^1 F\mathscr{L}(F)\,dt < 0,$$

which implies $\Lambda_1 < 0$. An example of such a Π_1^∞ and its associated trial function F is shown in figure 20. F is chosen to coincide with Π_1^∞ in the range it is negative and to be zero everywhere else except in a small region near each end-point, if necessary, to satisfy the boundary condition there. The amplitude of these end-point corrections (which may conveniently be formed from a portion of a sine curve) may be made arbitrarily small without altering the ratio F/F'; hence, their contribution to the integral

$$\int_0^1 F\mathscr{L}(F)\,dt$$

can be made vanishingly small. Furthermore, there will be no contribution from the neighbourhoods of the points on the θ-axis where F suddenly changes slope, since the value of the integral in such a neighbourhood is found (via an integration by parts) to equal the difference in slopes times the value of F at the point in question. Now F is equal to zero at the points of discontinuous slope, and

$\Pi_1^{\infty\prime}(\theta)$ must be finite for any physically interesting flow. Thus, the value of the integral is indeed zero at these points. Hence the integral I_R may be evaluated:

$$I_R = \int_0^1 F\mathscr{L}(F)\,d\theta = \int \Pi_1^\infty \mathscr{L}(\Pi_1^\infty)\,d\theta = \beta^* \int (\Pi_1^\infty/P_0)\,d\theta, \qquad \text{(A 12)}$$

where the last two integrals range only over regions of θ where $\Pi_1^\infty < 0$, and where use has been made of (A 3). It is clear that the Rayleigh integral is negative, which means there can be no boundary current. It is therefore concluded that

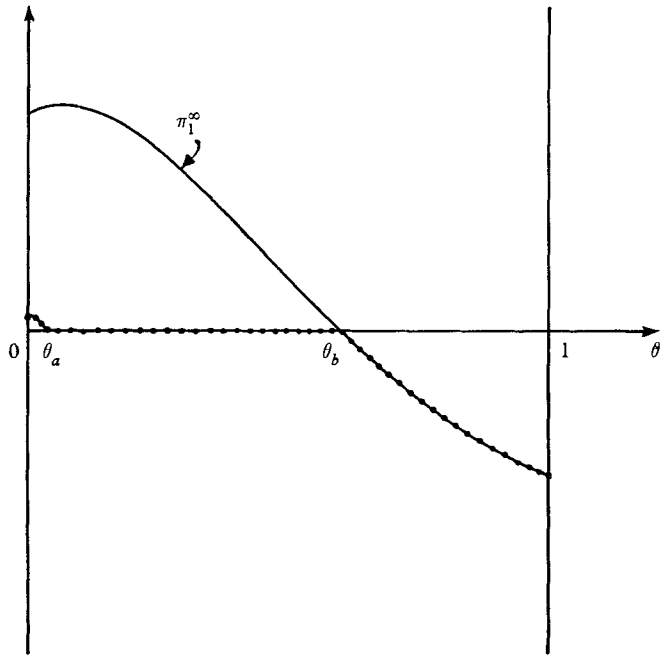

FIGURE 20. Example of a Π_1^∞ that changes sign (solid curve). A trial function $F(\theta)$ (dotted curve) is chosen to coincide with Π_1^∞ for its negative range ($\theta_b < \theta < 1$) and be zero elsewhere except for a small range near the endpoint ($0 < \theta < \theta_a$) where it may attain infinitesimal amplitude to satisfy the boundary condition. The Rayleigh integral $\int FF''P_0^{-1}\,d\theta$ will be negative for this F.

the presence of positive u_0^∞ at any level is inconsistent with achieving boundary-layer flow along the coast over a flat bottom. The only way to avoid this restriction is to permit infinite velocity gradients, which on physical grounds would imply the local importance of dissipative effects and thus be inconsistent with the purely inertial model, or to relax the requirement of stable stratification, since the positiveness of P_0 is crucial to the above argument. It may be noted that this derivation constitutes a proof that the Green's function for any S–L system having only positive eigenvalues is always positive.

The support of this work by the National Science Foundation, in part by Grant G-24903 (Atmospheric Sciences) and in part by Grant GP-3533 (Oceanic Dynamics) to Harvard University is gratefully acknowledged.

REFERENCES

CHARNEY, J. G. 1955 The Gulf-Stream as an inertial boundary layer. *Proc. Nat. Acad. Sci.* (*U.S.*) **41**, 731–40.

C.S.I.R.O. Aust. 1963 *Oceanogr. Cruise Rept.* no. 6.

FUGLISTER, F. C. 1960 *Woods Hole Oceanogr. Inst. Atlas Series* **1**.

GREENSPAN, H. P. 1962 A criterion for the existence of inertial boundary layers in oceanic circulation. *Proc. Nat. Acad. Sci.* (*U.S.*) **48**, 2034–9.

GREENSPAN, H. P. 1963 A note concerning topography and inertial currents. *J. Mar. Res.* **21**, 147–54.

ISELIN, C. O'D. 1936 A study of the circulation of the western North Atlantic. *Pap. Phys. Oceanogr. Meteor.* **4**, no. 4.

LIGHTHILL, M. J. 1949 A technique for rendering approximate solutions to physical problems uniformly valid. *Phil. Mag.* (Ser. 7), **40**, 1179–201.

NIILER, P. P. & SPIEGEL, S. L. 1968 Formation of an inertial current on a continental shelf. *J Mar. Res.* **26**, 13–23.

PEDLOSKY, J. 1965 A necessary condition for the existence of an inertial boundary layer in a baroclinic ocean. *J. Mar. Res.* **23**, 69–71.

ROBINSON, A. R. 1965 A three-dimensional model of inertial currents in a variable density ocean. *J. Fluid Mech.* **21**, 211–23.

ROBINSON, A. R. & NIILER, P. P. 1967 The theory of free inertial currents: I. Path and Structure. *Tellus*, **19**, 269–91.

SPIEGEL, S. L. 1966 Existence and structure of inertial boundary currents in a stratified ocean. Harvard University Ph.D. thesis (unpublished).

STOMMEL, H. 1965 *The Gulf Stream*, 2nd ed. Berkeley and Los Angeles: University of California Press; Cambridge University Press.